



BUDAPEST UNIVERSITY OF TECHNOLOGY AND ECONOMICS
FACULTY OF MECHANICAL ENGINEERING

NÓRA MÁRIA NAGY

Modeling the sound production of a novel organ pipe
construction with free reed

Supervisor:

Dr. Péter Rucz

Budapest, 2016

ABSTRACT

It is a known fact that traditional organ pipes can only be played in a strictly limited range of dynamics. Each pipe is designed and tuned to a given nominal windchest pressure. Modifying the pressure of the wind supply also affects the pitch and the timbre of the pipe. Therefore, unlike on the piano, the volume of the sound cannot be controlled by the strength or the velocity of pressing the keys.

In order to overcome these limitations, a German instrument maker proposed a new pipe construction that can handle changing wind supply and produce louder or quieter voice, depending on the pressure, while keeping the pitch of the pipe stable. On the other hand, as it was found from laboratory measurements, the timbre is changing significantly with the blowing pressure. In order to improve the design, we first need to establish a physical model of the voice production of this new construction, and set it against the results of the measurements.

In this thesis the sound generation of the novel pipe construction is simulated using various physical models. First, a brief review of the parts of the pipe organ is given as well as the explanation of the operation of two types of organ pipes: labial and lingual ones. Then the model of the sound production of the new organ pipe construction is elaborated. A coupled system of a free reed connected to a resonator is studied. The simulation of the interaction of these elements is carried out by means of two different methods. First, the model of truncated impedances is used, and second, the so-called reflection function approach is examined. Finally, the comparison of the results of the simulations and the measurements is presented and discussed in this paper.

KIVONAT

Ismert tény, hogy a hagyományos orgonasípok hangereje játék közben nem változtatható, hiszen mindegyik síp egy adott névleges nyomásértékre van tervezve. Ezen nyomás megváltoztatása kihat az orgonasíp hangmagasságára valamint hangszínére is. Így – a zongorával ellentétben – a hangerősség nem változtatható a billentyűk lenyomásának erejével.

A probléma orvoslására egy német hangszerkészítő mester új konstrukciót hozott létre, melynek lényege, hogy a sípok különböző nyomás esetén képesek hangosabban vagy halkabban megszólalni, míg a hangmagasságuk állandó marad. Azonban, ahogy azt korábbi mérések kimutatták, az új sípok hangszíne továbbra is érzékeny a megfűväs nyomására. A konstrukció javításának érdekében elöször fel kell állítani a sípok hangkeltésének fizikai modelljét és össze kell azt hasonlítani a mérések eredményével.

Jelen dolgozat bemutatja az újfajta sípok hangkeltésének két különböző modell alapján történő szimulációját. A dolgozat elöször ismerteti az orgona különböző részeit és kétfajta orgonasíp (az ajak-, valamint a nyelvcsíp) hangkeltési mechanizmusát. Ezután az új konstrukció hangkeltésének modellezésébe ad betekintést. A dolgozat tanulmányozza továbbá a rezgő nyelvöl és rezonátorból létrehozott csatolt rendszer viselkedését, ahol a rezgő nyelv egy speciális, úgynevezett „átcsapó nyelv”, mely egy egyik végén befogott rúdként modellezhető. A rendszer működését két különböző elv felhasználásával modellezzük: elöször a modális szuperpozíció elvét felhasználva, a bemenő impedancia segítségével, majd a reflexiós függvény módszerével. A dolgozatot a szimulációs eredmények egymással, valamint a méréssel való összehasonlítása és értékelése zárja.

ACKNOWLEDGEMENT

I would like to thank my supervisor, Dr. Péter Rucz for all the help, time and energy he provided during our work.

TABLE OF CONTENTS

Abstract.....	1
Kivonat	2
Acknowledgement.....	3
1. Introduction.....	6
1.1. Motivation	6
1.2. Objectives.....	6
2. Voice production of organ pipes	8
2.1. The pipe organ.....	8
2.2. Organ pipe constructions.....	10
3. Model of the sound production	14
3.1. General model	14
3.2. Model of the reed vibration.....	15
3.3. Model of the resonator	17
3.3.1. Sound propagation in ducts	17
3.3.2. Input impedance.....	19
3.3.3. Transfer matrix	20
3.3.4. Self and mutual impedance of the resonators.....	22
3.4. Flow model.....	26
3.4.1. Jet velocity.....	26
3.4.2. Useful section	28
4. Computer model.....	32
4.1. Reed vibration by modal superposition	32
4.2. Resonator representation.....	34
4.2.1. Modal superposition.....	34
4.2.2. Reflection function.....	35
4.3. Iterative solution.....	36
5. Results.....	37
5.1. Validation of the modeling methodology	37

5.1.1. Reed vibration.....	37
5.1.2. Resonator.....	38
5.1.3. Impedance truncation	39
5.1.4. Reflection function.....	40
5.1.5. Extremal cases	42
5.2. Simulation of the experimental pipes	46
5.2.1. Comparison of static parameters.....	46
5.2.2. Transient vibration	47
5.2.3. Impedance truncation versus reflection function.....	48
5.2.4. The effect of the truncation	50
5.2.5. Changing the blowing pressure.....	50
6. Conclusion	53
References.....	55

1. INTRODUCTION

1.1. Motivation

It is a known fact that traditional organ pipes can only be played in a strictly limited range of dynamics. [Miklós et al, 2003, 2006] Each pipe is designed and tuned to a given nominal windchest pressure. Modifying the pressure of the wind supply also affects the pitch and the timbre of the pipe. Therefore, unlike on the piano, the volume of the sound cannot be controlled by the strength or the velocity of pressing the keys. To be able to control the volume of the sound to some extent, the organ pipes can be arranged in a big wooden box, called the swell. One side of this box consists of palettes that can be closed or opened by a pedal. Therefore, when the palettes are closed, less sound is released. The disadvantage of this method is that the control over the volume is limited, moreover, as the wind supply has to be steady, it cannot be controlled by the musician. In grandiose church or concert organs that have a great number of stops the dynamics can also be controlled by turning stops on or off. However, in case of smaller pipe organs this is not an option due to the limited number of stops.

In order to overcome these problems, a German instrument maker has recently produced a new pipe construction that can handle changing wind supply and produce louder or quieter voice, depending on the pressure, while keeping the pitch of the pipe stable [Zacharias 2015]. On the other hand, as it was found from measurements carried out on experimental pipes the timbre is changing significantly with the blowing pressure [Rucz et al. 2016]. In order to improve the design, we need to establish a physical model of the voice production of this new construction, and set it against the results of the measurements.

1.2. Objectives

The present thesis aims at the establishment and analysis of the physical model by means of computer simulations. As the sound generation mechanism of lingual pipes is a very complex process involving coupled fluid flow, mechanical vibration and acousti-

cal phenomena, it is necessary to introduce simplifications in the computer model. In the thesis a “one-dimensional” arrangement is established and examined. The simplified model can be regarded as one-dimensional because of the following reasons.

First, wave propagation in the resonator is limited to the simulation of planar or spherical waves travelling along the axis of the pipe. This means a limitation to the applicable frequency range of the model, as discussed later. Second, the flow model is simplified by substituting the real three-dimensional setup by a one-dimensional description making use of effective quantities.

On the other hand, the reduced complexity of the model allows for rapid simulations and synthesis of sound samples by means of time domain computations. These computer simulations are helpful for assessing the correctness of the physical model. Moreover, results obtained from the computer simulations are expected to be helpful in explaining the tendencies observed in the measurements.

2. VOICE PRODUCTION OF ORGAN PIPES

2.1. *The pipe organ*

According to the Hornbostel – Sachs system, musical instruments can be categorized by the way they produce sound into 5 different groups.

- Idiophones – any musical instrument, that creates sound by the way of the instrument itself vibrating, without the use of membranes, strings or air columns as resonators
- Membranophones – the sound is created by a stretched membrane
- Chordophones – the sound is created by a stretched string
- Aerophones – the sound is produced by vibrating air
- Electrophones – the sound is produced with the help of electricity

According to this grouping, the pipe organ is an aerophone instrument as organ pipes produce sound by the vibrating air column enclosed in the resonator of the pipes.

The pipe organ has three main parts. The main units can be seen in Figure 1. The first part, which is used to play the instrument is called console (also known as keydesk). This part contains the manuals (keyboards) with the stop controls (registration) and the pedalboards. A usual church or concert organ has several (sometimes up to 4–5) manuals and at least one pedalboard. The musical range of an average organ is 7–8 octaves or sometimes even more. The stops select which pipes are sounded when a key or pedal is pressed. Hence the player can modify the timbre and the volume of the instrument by using different combination of the stops.

The second part, often referred to as action ensures the connection between the sound producing element and the console. The first system of moving parts admits wind into the proper key channel when a key is pressed. This mechanism is called rollerboard. The other system (also called “stop”) allows the organist to control which ranks are engaged. According to their operation, the systems of moving parts can be mechanic, pneumatic, electric, or some combination of these.

The sound producing element of the pipe organ consists of the pipes and the wind system. The wind system has three parts: the blower, the regulator and the wind duct. There are several sets of pipes, with different timbre. One set of pipes having the same form

and timbre and arranged in a musical scale is called a pipe rank. The ranks are mounted vertically onto a windchest. Organ pipes can be divided into two main groups based on their sound production mechanism: labial (also known as flue) pipes and lingual (also known as reed) pipes.

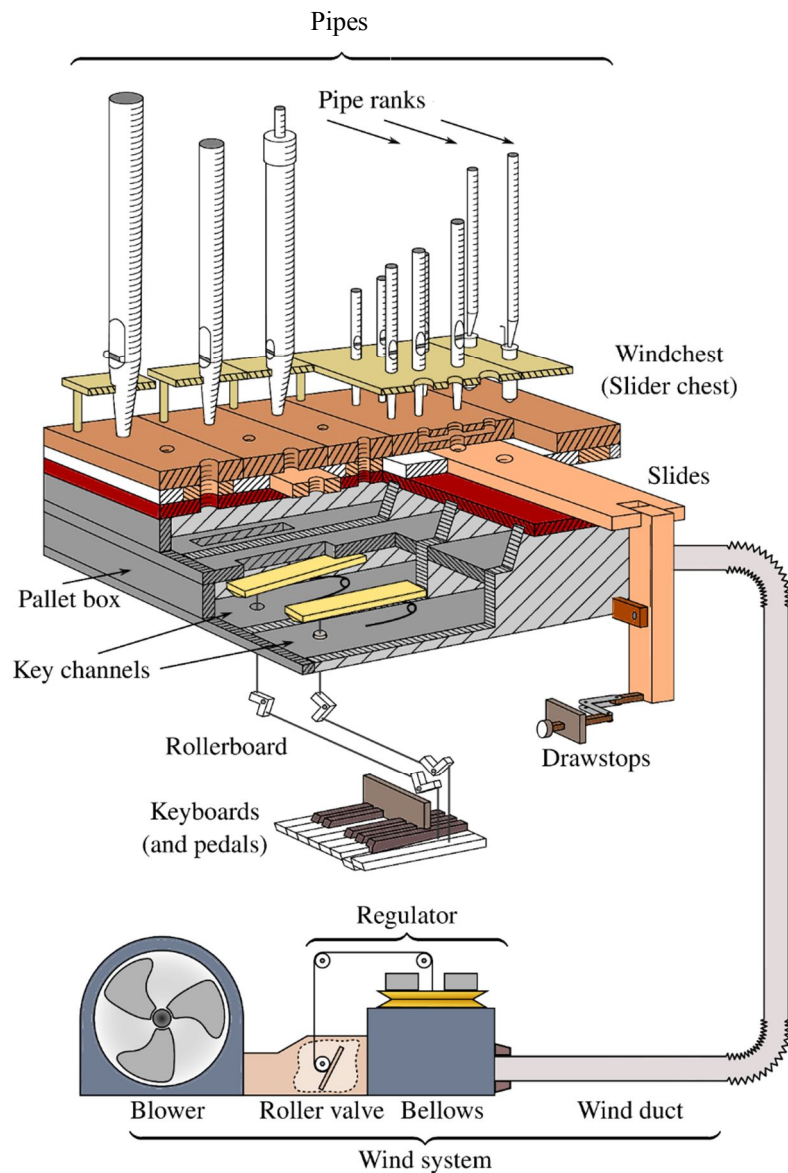


Figure 1. Parts of a pipe organ (source: [Rucz 2015])

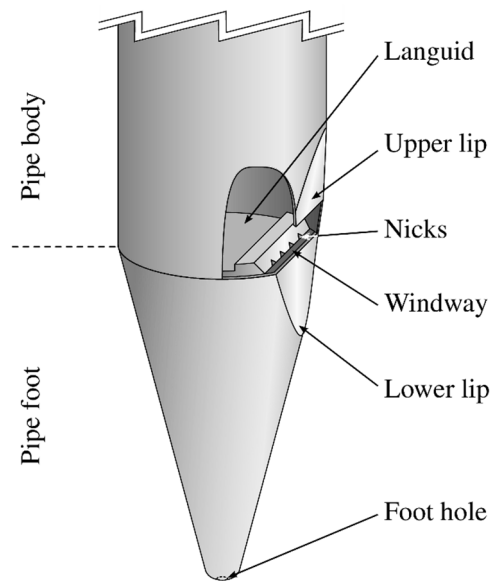


Figure 2. Labial pipe (source: [Rucz 2015])

2.2. Organ pipe constructions

The labial pipe can be seen in Figure 2. This type of pipe is winded through the foot hole, and the foot. The way of the air is blocked by the languid, therefore the wind passes through the windway as a thin jet. As the jet hits the lip, it becomes unstable and eddies are deflecting in a quasiperiodic manner. This causes an oscillation that excites the air column inside the resonator of the pipe. In the steady state of the sound generation constant amplitude is maintained by the balance of the energy entrained into the pipe, the radiated sound energy and different types of losses. The properties of the sounds of flue organ pipes and their physical explanations are reviewed by Miklós & Angster [Miklós, Angster 2000].

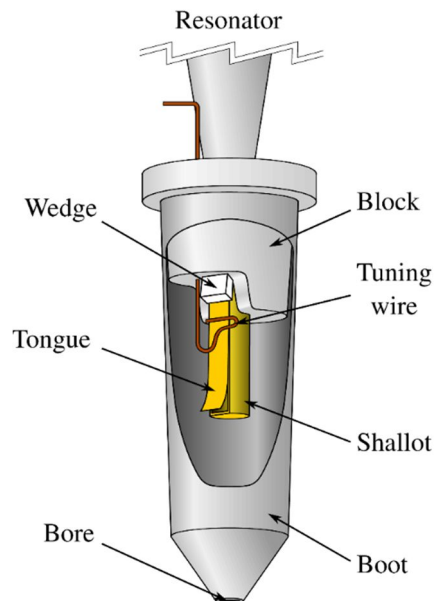


Figure 3. Structure of a lingual pipe (source: [Rucz 2015])

In case of lingual organ pipes (Figure 3) a vibrating reed (tongue) produces the sound. The reed is a flexible bar that is clamped at one end and free at the other end. The reed is usually a plate made by metal, namely brass in most cases. It usually has a little curvature, made by the instrument maker in a delicate procedure referred to as "curving". When the wind enters the pipe, the pressure increases inside the pipe foot and pushes the reed towards the shallot. At the same time, air flows through the small gap between the shallot and the reed, and the Bernoulli force also pulls the tongue in the same direction. After the pressure equalization the elasticity of the reed forces it back to its original position and the procedure starts over. The acoustic feedback of the resonator can amplify the oscillation of the reed, creating a stable and strong sound in the steady state. The instrument usually oscillates close to the natural frequency of the reed. [Miklós et al. 2003 és Miklós et al. 2006]

The reeds of lingual pipes can be grouped based on the construction of the shallot. There are so-called beating reeds, and free reeds. A beating reed hits the edges of the frame to which it is attached in each period of its oscillation, and it is not allowed to bend over the frame. Beside organ pipes, beating reeds are also used in woodwind instruments, for example in clarinets and saxophones. On the other hand, in case of a free reed, the reed is allowed to go through the frame. It is used e.g. in the harmonica, harmonium, melodica and bandoneon.

The reeds can also be grouped based on the initial position of the reed. The first type is the blown closed reed, which means, that the reed is initially open, and the exciting pressure forces move it closer to the frame. If the blowing pressure is increased above a critical level, the reed closes the way of air completely, hence the term “blown closed”. This type of reed is mainly used in woodwind instruments. The other type of reed operates the opposite way. It is initially closed or nearly closed, and the pressure pushes it away from the support. It is called the blown open reed. This type of reed is used in a harmonica. Fletcher developed a model of pressure-controlled valves in gas flows [Fletcher, 1993]. He treated the valves equivalent to the blown closed and blown open reeds. He used the analogue network of the valves to analyse the system, in which the current equals the volume velocity, the voltage equals the pressure. Therefore the impedances can be calculated the same way as in case of an electrical circuit. The same analogue model will be used in this paper to calculate the input and output impedances of the pipes.

The new construction we are studying is displayed in Figure 4. It is a special type of lingual pipe: a pipe with a free reed. As it does not have a shallot, the construction of the pipe is much simpler than that of traditional reed pipes. Unlike the previous construction, these lingual pipes operate with the help of a blown open reed instead of a blown closed one. There is a window on the experimental pipes made of plexiglas. The vibration of the reed can be measured through it using a laser vibrometer. The pipes can be built with different resonator shapes, as shown also in Figure 4.

In this thesis, three experimental pipes with very different resonators are examined. The first pipe has a simple, straight resonator that is open at both ends. The second pipe also has a straight resonator, open in both ends, but it is turned into half, therefore the two ends are located side by side and are in a stronger interaction. The third pipe has a conical resonator with one open end. This resonator is also turned into half.

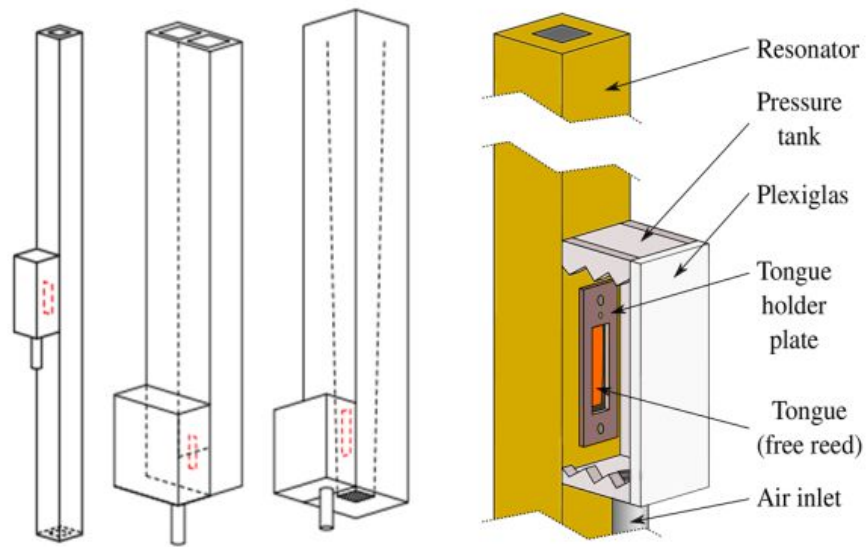


Figure 4. Construction of the studied experimental pipes. Left: Different resonator shapes. Right: The free reed in the new construction. The place of the reeds are marked with red dashed lines.

3. MODEL OF THE SOUND PRODUCTION

3.1. General model

In case of linear systems modal superposition is the most effective way of modelling the instrument. Thus, modal superposition is also often applied in practice for sound synthesis purposes. The eigenfrequencies and eigenmodes of a vibrating system can be easily calculated if the system is not time dependent. On the other hand, in case of time dependent and nonlinear influences, the procedure is much more difficult. As the sound production of aerophone musical instruments also contains nonlinear elements, McIntyre et al. have developed a simplified model [McIntyre et al. 1983]. According to this model the sound production can be described by the system of a nonlinear and a linear element. A submodel of the nonlinear excitation element has to be elaborated, which is connected to a submodel of the linear passive element, i.e. the resonator. By coupling the two models, the model of the whole system is obtained (Figure 5).

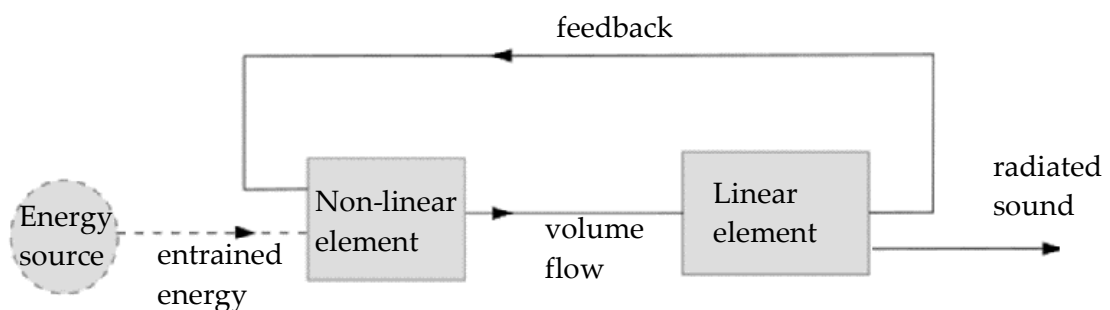


Figure 5. The McIntyre–Woodhouse–Schumacher model of sound production in musical instruments

In our case, the nonlinear elements are the oscillation of the exciting reed and the air-flow under the reed, the linear element is the resonator. In the sequel the physical description of these subsystems are discussed in detail.

3.2. Model of the reed vibration

The oscillating reed in the lingual pipes can be modelled by a free–clamped beam. In this case, the bending vibrations can be calculated from the reed motion equation that can be defined with the help of the Euler–Bernoulli beam theory, Newton’s second law and Hooke’s law. The equation of motion of the Euler–Bernoulli beam reads as

$$g(x, t) - (E \cdot I(x) \cdot u''(x, t))'' = \rho \cdot A(x) \cdot \ddot{u}(x, t), \quad (1)$$

where:

- $g(x, t) \left[\frac{\text{N}}{\text{m}} \right]$: external force per unit length
- E [Pa]: Young’s (or elastic) modulus of the reed
- I [m⁴]: second moment of area of the reed
- $u(x, t)$ [m]: transversal displacement of the reed
- $\rho \left[\frac{\text{kg}}{\text{m}^3} \right]$: density of the reed
- A [m²]: cross section of the reed

Using the Euler–Bernoulli assumption we assume that

- There is one section of the beam that does not suffer from compression or extension. It is called as neutral section.
- The cross section of the beam is perpendicular to the neutral section along the whole length of the beam during the motion.

The dot notation refers to the derivative with respect to time t and the apostrophe to the derivative with respect to the spatial coordinate x .

This differential equation can be solved using four boundary conditions. In this case, one end (at $x = 0$) of the beam is clamped and the other end (at $x = L$) is hanging freely. Thus, the boundary conditions are:

- $u(0) = 0$ this boundary condition states that the clamped end of the beam does not experience any deflection
- $u'(0) = 0$ as $u'(x)$ indicates the slope of the beam along the length, this boundary condition says, that the beam cannot bend at the clamped end
- $u''(L)=0$ this boundary condition says, that there is no bending moment at the free end of the reed

- $u'''(L) = 0$ this boundary condition says that no shear forces act at the free end of the reed

Solving the equation of motion using the boundary conditions above, we get the following transcendental equation for the wavenumber k :

$$\cos(kL) = \frac{-1}{\text{ch}(kL)} \quad (2)$$

After solving this equation (using a graphical method), the wavenumbers are found as

$$k_n = \frac{\pi}{2L} [1.194; 2.985; 5; 7; 9; \dots] \quad (3)$$

The eigenfrequencies:

$$\omega_n = c_L \cdot K \cdot \frac{\pi^2}{4L^2} [1.194^2; 2.985^2; 5^2, 7^2, 9^2 \dots] \quad (4)$$

Where K is the radius of gyration $K = \sqrt{\frac{I}{A}}$ [m] and c_L is the propagation speed of longitudinal waves in the material $c_L = \sqrt{\frac{E}{\rho}}$ $\left[\frac{\text{m}}{\text{s}}\right]$.

The eigenmodes:

$$\begin{aligned} \psi_n(x) = & A_n \cdot [\sin(k_n x) - \text{sh}(k_n x)] - \\ & A_n \cdot \frac{\sin(k_n L) + \text{sh}(k_n L)}{\cos(k_n L) + \text{ch}(k_n L)} \cdot [\cos(k_n x) - \text{ch}(k_n x)] \end{aligned} \quad (5)$$

The modes are linearly independent, as none of the eigenmodes can be defined as a linear combination of the others. Furthermore, the modes are orthogonal, (which means that the scalar product of ψ_n and ψ_m equals to zero if $n \neq m$ and a positive scalar if $n = m$) and normalized by choosing the constants A_n appropriately.

The vibration of the reed can be written as the superposition of the eigenmodes:

$$u(x, t) = \sum_{n=1}^{\infty} \alpha_n(t) \cdot \psi_n(x) \quad (6)$$

where α_n is the time dependent weight of the ψ_n eigenmode, also known as the modal coordinate. This form is referred to as modal superposition. There is an ω_n eigenfrequency to every ψ_n eigenmode. In case of undamped, free vibration, the ψ_n eigenmode is oscillating with this frequency. Thanks to the orthogonality of the eigenmodes the modal superposition form (6) decouples the equation of motion a system consisting of independent harmonic oscillators, as discussed in Section 4.1.

3.3. Model of the resonator

3.3.1. SOUND PROPAGATION IN DUCTS

In order to elaborate the model of the resonator, the differential equation of sound propagation has to be defined. To attain the 3D wave equation we assume that the propagation of sound waves is a frictionless, adiabatic process. We also assume that the medium (air in our case) is an ideal gas. The governing equations of the sound field have to be linearized by writing the variables as a superposition of a location and time independent part and a time and location dependent part. For example: the pressure can be divided into the constant atmospheric pressure P_0 and the location and time dependent sound pressure $p(\mathbf{x}, t)$:

$$P(\mathbf{x}, t) = P_0 + p(\mathbf{x}, t) \quad (7)$$

The first equation of the sound field is attained from Newton's second law as [Fiala, 2015]:

$$\nabla p(\mathbf{x}, t) + \rho_0 \cdot \dot{\mathbf{v}}(\mathbf{x}, t) = 0 \quad (8)$$

where

- $\mathbf{v} \left[\frac{\text{m}}{\text{s}} \right]$ is the vector of the particle velocity.
- $\rho_0 \left[\frac{\text{kg}}{\text{m}^3} \right]$ is the average equilibrium density of the fluid
- $p(\mathbf{x}, t)$ [Pa] is the sound pressure

The second equation of the sound field is derived from the equation of state of an ideal gas undergoing an adiabatic process:

$$p(\mathbf{x}, t) = -\kappa P_0 \nabla \cdot \mathbf{u}(\mathbf{x}, t) \quad (9)$$

where κ is the specific heat capacity and \mathbf{u} is the particle displacement.

The 3D wave equation can be deduced as the combination of the divergence of the first equation and the second time derivative of the second equation of the sound field.

$$\nabla \cdot \nabla p(\mathbf{x}, t) = \frac{1}{c^2} \ddot{p}(\mathbf{x}, t) \quad (10)$$

where $c = \sqrt{\frac{\kappa P_0}{\rho_0}} \left[\frac{\text{m}}{\text{s}} \right]$ is the speed of sound in the given fluid.

In case of time harmonic vibration, the wave equation can be written as the Helmholtz equation in the following form:

$$\nabla^2 p + k^2 p = 0 \quad (11)$$

Where $k = \frac{\omega}{c} \left[\frac{1}{\text{m}} \right]$ is the wavenumber.

In case of a cylindrical duct, this equation can be written in a cylindrical coordinate system (r, θ, x) :

$$\frac{\partial^2 p}{\partial r^2} + \frac{1}{r} \frac{\partial p}{\partial r} + \frac{1}{r^2} \frac{\partial^2 p}{\partial \theta^2} + \frac{\partial^2 p}{\partial x^2} + k^2 p = 0 \quad (12)$$

The solution of this equation shows, that the function that describes the waves in a cylindrical duct consists of the multiplication of radial, tangential and longitudinal waves [Fletcher & Rossing 1998, chapter 8]. The radial components can be described by the Bessel functions, the tangential components are harmonic functions and the longitudinal ones are plain waves. There is a certain frequency, called cut-off frequency, for every radial and tangential mode, above which the waves are propagating waves. Under this frequency, the waves are evanescent and they are decaying exponentially near the excitation along the x axis. In case of the radially and tangentially constant modes, this frequency is zero, which means, that propagating plane waves can evolve at any frequency. The first non-planar mode with the lowest cut-off frequency is the first tangential (also called as transverse) mode. The limit frequency of this eigenmode is called the cut-off frequency of the duct.

The musically relevant frequency range of organ pipes is below the cut-off frequency of their resonators, therefore the plain wave model is used in the further deductions, and the radial and tangential eigenmodes are neglected.

The one-dimensional form of the wave equation:

$$p''(x, t) = \frac{1}{c^2} \ddot{p}(x, t) \quad (13)$$

The one-dimensional form of the Helmholtz equation:

$$p''(x, t) + k^2 p(x, t) = 0 \quad (14)$$

The general solution of this equation in a complex form reads as

$$p^+ e^{-jkx} + p^- e^{+jkx} \quad (15)$$

where p^+ and p^- are the complex amplitudes of the ingoing and outgoing plain waves.

According to equation (8), the connection between the sound pressure and the particle velocity:

$$v(x) = -\frac{1}{j\omega\rho_0} p'(x) = \frac{jkp(x)}{j\omega\rho_0} = \frac{p(x)}{c\rho_0} = \frac{p(x)}{z_0} \quad (16)$$

Where $z_0 = c\rho_0$ is the specific impedance of the plane wave.

The specific impedance expresses the connection between the pressure and the velocity:

$$z = \frac{p(x)}{v(x)} \quad (17)$$

3.3.2. INPUT IMPEDANCE

Substituting formula (15) into equation (8) the ratio of the pressure and the velocity can be expressed as

$$z(x) = \rho_0 c \frac{p^+ e^{-jkx} + p^- e^{+jkx}}{p^+ e^{-jkx} - p^- e^{+jkx}} \quad (18)$$

It can be also expressed in the following form:

$$z(x) = \rho_0 c \frac{1 + R e^{2jkx}}{1 - R e^{2jkx}} \quad (19)$$

Where R is the reflection coefficient:

$$R = p^- / p^+ \quad (20)$$

An other form of the reflection coefficient reads as

$$R = \frac{z_2 - z_0}{z_2 + z_0} e^{-jkL} \quad (21)$$

Where $z_2 = z(L)$ is the termination impedance of the pipe at $x = L$. The latter formula is of great use in our applications for calculating the input impedance of resonators.

The input impedance of a duct shows the relationship between the sound pressure and the particle velocity at $x = 0$. The natural resonance frequencies and the damping of the system can be evaluated by examining this connection, as discussed in the following.

The impedance at $x = 0$ can be expressed if the reflection coefficient (or the termination impedance) is known:

$$z_{in} = z(0) = z_0 \frac{1+r}{1-r} = z_0 \frac{z_2 \cdot \cos(kL) + jz_0 \cdot \sin(kL)}{jz_2 \cdot \sin(kL) + z_0 \cdot \cos(kL)} = z_0 \frac{z_2 + jz_0 \cdot \tan(kL)}{z_0 + jz_2 \cdot \tan(kL)} \quad (22)$$

If the pipe is ideally closed at the input side, the velocity at $x = 0$ also equals zero. In this case the pressure at $x = 0$ can be finite when we reach the eigenfrequency of the pipe, therefore the input impedance of the resonator is infinite. That means that the eigenfrequencies of the pipe are assigned by the impedance function's singular points. If the resonator is excited by a reed at $x = 0$, the velocity is not zero, but the eigenfrequencies are still assigned by the local maxima of the input impedance function. This

statement can be explained by the fact that the pressure response (acoustic feedback) to an excitation is maximal in case of a natural resonance. The quality factors (Q factors) of the eigenmodes (and therefore the damping of the duct) can be calculated using the half power bandwidth method shown in Figure 6.

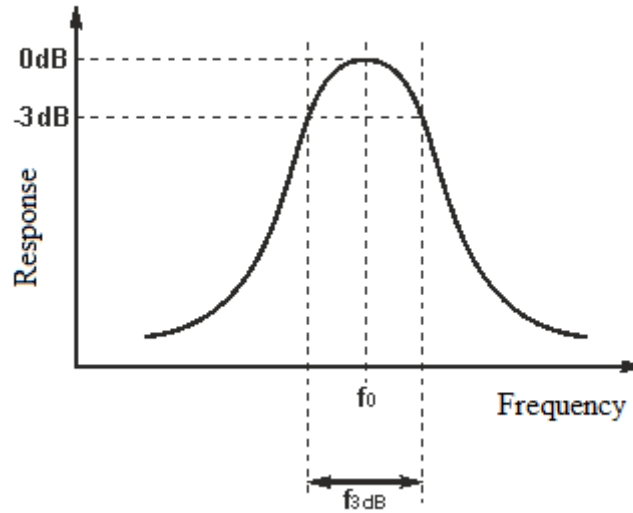


Figure 6. Half power bandwidth method for calculating the Q factors.

$$Q = \frac{f_0}{f_{3dB}} = \frac{1}{2 \cdot \xi} \quad (23)$$

Where ξ is the damping factor. The quality factor also indicates the energy losses of the system: for example the radiation losses (this is the produced sound, but interpreted as a loss from the resonator's point of view). This loss is indicated by the real part of the radiation impedance (or output impedance) of the resonator.

Another relevant source of energy loss is called “wall loss” or “viscothermal loss”. In case of wave propagation, there is friction and heat transfer between the walls and the particles of the medium, and therefore energy loss occurs. These effects will be taken into consideration in the further calculations, and will have a great influence on the quality factor of the examined resonators. [Kinsler et al, 2000, chapter 8].

3.3.3. TRANSFER MATRIX

The parameters of a simple duct can be calculated using the formulas of the previous section; however, in case of composite resonators the description of a complex system is

needed. The calculation of the parameters of a resonator that consists of more elements (even of conical parts) is addressed in the following section.

The connection between the input and output pressure (p_{in} and p_{out}) and volume velocity (U_{in} and U_{out}) can be expressed in the following form [Rucz, 2015]:

$$\begin{bmatrix} p_{in} \\ U_{in} \end{bmatrix} = \begin{bmatrix} T_{11} & T_{12} \\ T_{21} & T_{22} \end{bmatrix} \cdot \begin{bmatrix} p_{out} \\ U_{out} \end{bmatrix} \quad (24)$$

Where the frequency dependent matrix \mathbf{T} is the transmission matrix of the resonator.

Using the transmission matrix, equations of complex systems can also be defined if we equate input parameters of the given system and the output parameters of the other system.

$$\begin{bmatrix} p_{in} \\ U_{in} \end{bmatrix} = \left[\prod_{i=1}^N \mathbf{T}_i \right] \cdot \begin{bmatrix} p_{out} \\ U_{out} \end{bmatrix} \quad (25)$$

where the resultant transmission matrix: $\mathbf{T}_e = \prod_{i=1}^N \mathbf{T}_i$

If the impedance at $x = L$ is known, the transfer impedance (p_{out}/U_{in}) or the input impedance of the system can be calculated.

The transfer matrix of a cylindrical duct is obtained as:

$$\begin{bmatrix} p(x_1) \\ U(x_1) \end{bmatrix} = \begin{bmatrix} \cos kL & jZ_0 \sin kL \\ j\frac{1}{Z_0} \sin kL & \cos kL \end{bmatrix} \cdot \begin{bmatrix} p(x_2) \\ U(x_2) \end{bmatrix} \quad (26)$$

Where:

- $x_2 = x_1 + L$
- $Z_0 = \frac{c\rho_0}{S}$ is the acoustic plane wave impedance of the duct with S denoting the cross section area of the duct

If a termination impedance $Z_L(\omega)$ is assumed at $x = L$, the input impedance can be expressed in the following form:

$$Z_{in}(\omega) = \frac{p(x_1)}{U(x_1)} = \frac{Z_L(\omega) \cdot T_{11} + T_{12}}{Z_L(\omega) \cdot T_{21} + T_{22}} \quad (27)$$

The transfer matrix of conical ducts can be determined in the same way [Olson, 1960]

$$T_{cone}(kL) = \begin{bmatrix} -m \frac{\sin(kL - \theta_{out})}{\sin \theta_{out}} & jm \frac{1}{Z_{0,out}} \sin(kL) \\ jm Z_{0,in} \frac{\sin(kL + \theta_{in} - \theta_{out})}{\sin(\theta_{in}) \cdot \sin(\theta_{out})} & \frac{1}{m} \cdot \frac{\sin(kL - \theta_{in})}{\sin \theta_{in}} \end{bmatrix} \quad (28)$$

where:

- $m = \frac{r_L}{r_0}$: the ratio of input and output radii
- $Z_{0,in} = \frac{\rho_0 c}{r_0^2 \pi}$ the plane wave impedance at $x = 0$

- $Z_{0,out} = \frac{\rho_0 c}{r_L^2 \pi}$ the plane wave impedance at $x = L$
- $\theta_{in} = \tan^{-1}(k \cdot x_{in})$ the angle at the input
- $\theta_{out} = \tan^{-1}(k \cdot x_{out})$ the angle at the output
- x_{in} the distance of the cone's input plane from the apex
- x_{out} the distance of the cone's output plane from the apex

If $r_L = r_0$ the transfer matrix equals the transfer matrix of the cylindrical duct. In case of an axisymmetric composite duct the resulting transfer matrix can be calculated as the product of the sections' transfer matrices, see equation (25).

In the following chapters the transfer matrix method is utilized for calculating the input impedance function of different resonators in order to attain their eigenfrequencies and reflection properties.

3.3.4. SELF AND MUTUAL IMPEDANCE OF THE RESONATORS

If the resonator has two open ends the parameters of the system cannot be calculated using just the simple input impedance of the resonator, as the two resonator parts are coupled through their open end. P. Rucz developed a method of calculating these systems with the help of a coupling impedance matrix. [Rucz, 2016] He used the finite element method (FEM) for constructing the coupling impedance matrix of the resonators and applied it in the one dimensional waveguide model. The analogue network of a reed driven resonator with two coupled ends can be seen in Figure 7. The reed is modelled as a volume velocity source, providing the input velocity U_{in} .

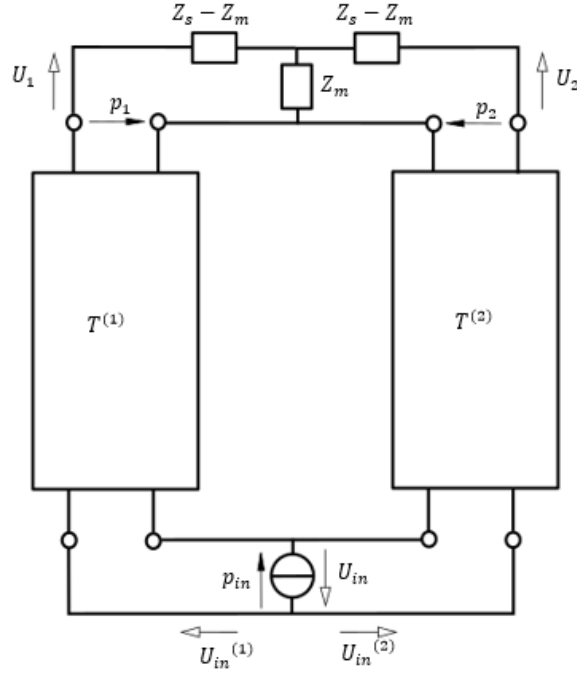


Figure 7. Analogue network of a resonator with coupled ends

The acoustical impedance matrix relates the pressure and volume velocities:

$$\mathbf{p} = \mathbf{Z} \cdot \mathbf{u}$$

In this case:

$$\begin{bmatrix} p_1 \\ p_2 \end{bmatrix} = \begin{bmatrix} Z_{11} & Z_{12} \\ Z_{21} & Z_{22} \end{bmatrix} \cdot \begin{bmatrix} U_1 \\ U_2 \end{bmatrix} \quad (29)$$

Where Z_{11} and Z_{22} are the self-impedances, and Z_{21} , and Z_{12} are the mutual impedances.

$T^{(1)}$ and $T^{(2)}$ are the transfer matrices of the resonators. As the input pressures of the two resonators are the same, the relationship between the input quantities and output quantities can be written in the form of equation (24):

$$\begin{bmatrix} p_{in} \\ U_{in}^{(i)} \end{bmatrix} = \begin{bmatrix} T_{11}^{(i)} & T_{12}^{(i)} \\ T_{21}^{(i)} & T_{22}^{(i)} \end{bmatrix} \cdot \begin{bmatrix} p_i \\ U_i \end{bmatrix} \quad (i = 1, 2) \quad (30)$$

The continuity of the volume velocity can also be seen in Figure 7.

$$U_{in}^{(1)} + U_{in}^{(2)} = U_{in} \quad (31)$$

Equation (29), (30) and (31) can be separated into 7 scalar equations, and as there are 7 unknowns ($p_1, U_1, p_2, U_2, p_{in}, U_{in}^{(1)}, U_{in}^{(2)}$) As U_{in} can be determined from the reed vibration, the impedance matrix is defined using the FEM and the transfer matrix of the resonators can be expressed according to section 3.3.3.

After solving the system of equations, the input impedance can be calculated:

$$Z_{in} = \frac{p_{in}}{U_{in}} \quad (32)$$

The radiated pressure:

$$p_{rad} = Z_s \cdot (U_1 + U_2) \quad (33)$$

Thus, the transfer function (that relates the output pressure and the input volume velocity):

$$H = \frac{p_{rad}}{U_{in}} \quad (34)$$

Simulations show, that in the low frequency range, the coupling impedance does not have a huge impact on the input impedance of the resonator. The frequencies of the peaks are slightly shifted down and the amplitudes of the peaks are decreasing due to the coupling. At higher frequencies, the effects are more significant.

On the other hand, the transfer function is affected highly by the coupling, as the volume velocities of the two resonator parts have opposite signs. The even peaks are disappearing from the transfer function, and the odd peaks are increasing.

In case of an uncoupled system, the acoustical network can be seen Figure 8.

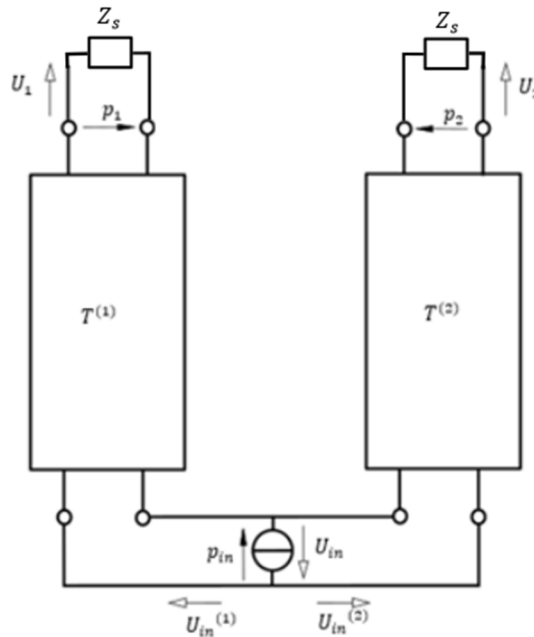


Figure 8. Network of a resonator with uncoupled open ends

In this case, the radiated pressure equals to p_1 and p_2 can be calculated according to equation (30).

$$\begin{bmatrix} p_{in} \\ U_{in}^{(1)} \end{bmatrix} = \begin{bmatrix} T_{11}^{(1)} & T_{12}^{(1)} \\ T_{21}^{(1)} & T_{22}^{(1)} \end{bmatrix} \cdot \begin{bmatrix} p_1 \\ U_1 \end{bmatrix} \quad (35)$$

$$p_{in} = T_{11} \cdot p_1 + T_{12} \cdot \frac{p_1}{Z_s} = p_1 \cdot \left(T_{11} + \frac{T_{12}}{Z_s} \right) \quad (36)$$

The transfer function for the pressure (T_{rp}) is the ratio of p_1 and p_{in}

$$T_{rp}(\omega) = \frac{Z_s}{T_{11} \cdot Z_s + T_{12}} \quad (37)$$

The output pressure can be calculated in time domain by a convolution

$$p_1(t) = p_{out}(t) = p_{in}(t) * t_{rp} = \int_0^t p(\tau) \cdot t_{rp}(t - \tau) d\tau \quad (38)$$

Where t_{rp} is the inverse Fourier transform of the transfer function $T_{rp}(\omega)$

$$t_{rp}(t) = \frac{1}{2\pi} \int_{-\infty}^{\infty} T_{rp} \cdot e^{j\omega t} d\omega \quad (39)$$

If the pipe is closed at one end, the self-impedance at that end is considered infinite:

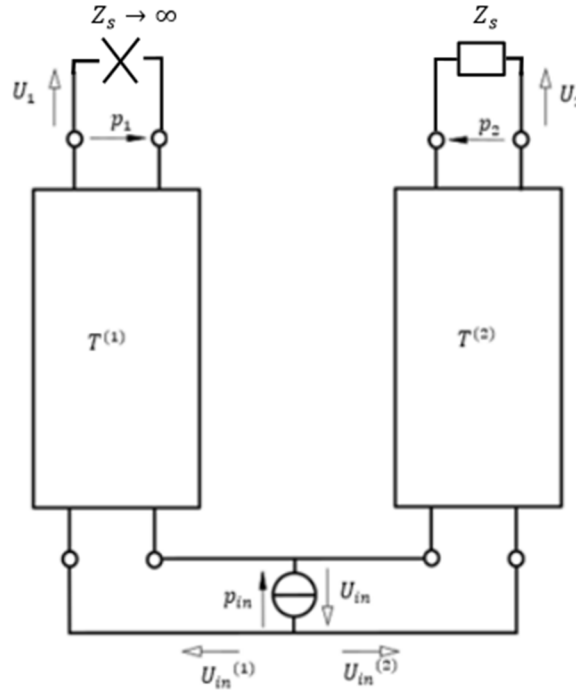


Figure 9. Resonator with a closed and an open end

In this case U_2 is zero, therefore, according to equation (30):

$$p_1 = T_{11} \cdot p_2 \quad (40)$$

$$U_1 = T_{21} \cdot p_2 \quad (41)$$

Therefore, the input impedance of the resonators:

$$Z_{in} = \frac{T_{11}}{T_{21}} \quad (42)$$

3.4. Flow model

3.4.1. JET VELOCITY

For the calculations of the air flow a simplified, one-dimensional flow model is used, because the real, three-dimensional model cannot be described by simple equations, and very expensive numerical simulations would be needed to arrive at approximate solutions. The one-dimensional description is also used by other authors, see for example [Adachi and Sato, 1995; Millot and Baumann, 2007]

In this model, Bernoulli's principle is used for describing the airflow. This principle states, that if the velocity of the fluid increases, the pressure or the potential energy of the fluid decreases.

If the flow is steady, the fluid is incompressible, and the viscous forces due to friction are negligible, Bernoulli's equation can be written in the following form:

$$\frac{v^2}{2} + gz + \frac{p}{\rho_0} = \text{constant} \quad (43)$$

where

- v is the fluid flow speed at a point on a streamline
- g is the acceleration due to gravity
- z is the elevation of the point above a reference plane (with the positive z direction pointing opposite the gravitational acceleration)

In the studied case, the Reynolds number is around the order of magnitude of a few thousands, which means that the viscous forces are much smaller than the inertial forces. Moreover, the air jet evolves in much less time than the period of the reed vibration. Therefore, the flow is considered steady, formula (43) can be used. As the velocity of the jet is significantly smaller than the speed of sound, the air is considered incompressible.

Bernoulli's equation can be written between the points '0' and '1' marked in Figure 10.

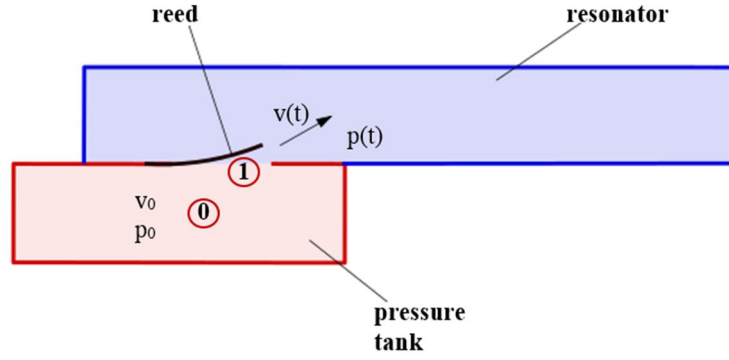


Figure 10. Illustration of the application of Bernoulli's law in the studied geometry

$$\rho_0 \cdot \frac{v_0^2}{2} + \rho g z_0 + p_0 = \rho_0 \cdot \frac{v(t)^2}{2} + \rho g z + p(t) \quad (44)$$

In this case there is no significant elevation between the examined points ($h_0 \approx h_1$), and the velocity of the jet is zero at point '0' therefore, the equation can be simplified:

$$p_0 = \rho_0 \cdot \frac{v(t)^2}{2} + p(t) \quad (45)$$

The velocity of the jet can be expressed in the following form:

$$v(t) = \sqrt{\frac{2}{\rho_0}} \sqrt{p_0 - p(t)} \cdot \text{sign}(p_0 - p(t)) \quad (46)$$

The volume flow passing under the reed can be calculated if the velocity is known.

$$U(t) = \alpha \cdot S_u(t) \cdot v(t) \quad (47)$$

Where

- S_u is the useful section—the section where the flow can pass through the gap formed by the moving reed and the tongue holder plate.
- α is the vena contracta coefficient

The vena contracta coefficient expresses the reduction of the area of a fluid jet emerging from a small aperture in a pressurized reservoir. The reduction of the area is explained by the flow separating from the sharp edges of the boundary, as the streamlines are unable to closely follow these edges. The point of the fluid stream, where the diameter of the stream is the smallest is called vena contracta.

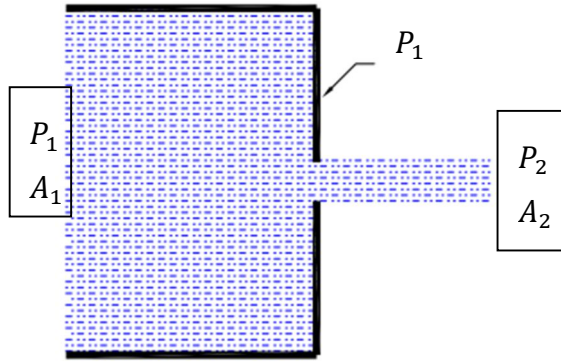


Figure 11. Theoretical jet

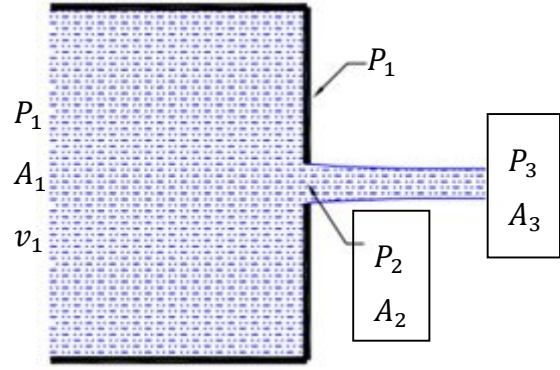


Figure 12. Vena contracta

The vena contracta coefficient takes this contraction of the jet into account, as illustrated in Figures 11 and 12.

$$\alpha = \frac{A_3}{A_2}$$

Where A_3 is the area at vena contracta, A_2 is the area of orifice. Experiments and theoretical analysis confirms [Hirschberg et al., 1990] that the vena contracta coefficient is in the range $0.5 < \alpha < 0.65$. It is worth noting that the vena contracta effect also appears in the windway of labial pipes. Vaik and Paál found by simulations that the contraction coefficient is around $\alpha \approx 0.77$ in this case [Vaik and Paál, 2013].

3.4.2. USEFUL SECTION

A model of a blown open reed can be seen in Figure 13.

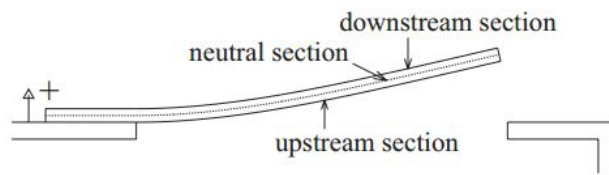


Figure 13. Model of a blown open reed following Millot & Baumann, 2007.

The ‘upstream section’ expression is used for the face that is in front of the pressure tank of the instrument, the ‘downstream section’ expression is used for the section that faces the resonator. To a first approximation the useful section can be calculated with the following formula:

$$S_u(t) = |h(t)| \cdot b \quad (48)$$

Where

- b is the width of the reed

- $h(t)$ is the reed opening at the upstream section, that can be calculated from the reed vibration

That means, that the air issues from the pressure tank only by the front section of the reed. This simplification is suitable for describing beating reeds of woodwind instruments (for example the reed of the clarinet or the saxophone). It is used in many papers and publications, see for example [Schumacher, 1981, Hirschberg, 1990, Gazengel, 1995]. In the first simulations, this approximation will be used.

However, to get more accurate results, the side areas need to be included in the calculations. The useful section can be calculated using the model of Millot and Baumann [Millot, Baumann, 2007]

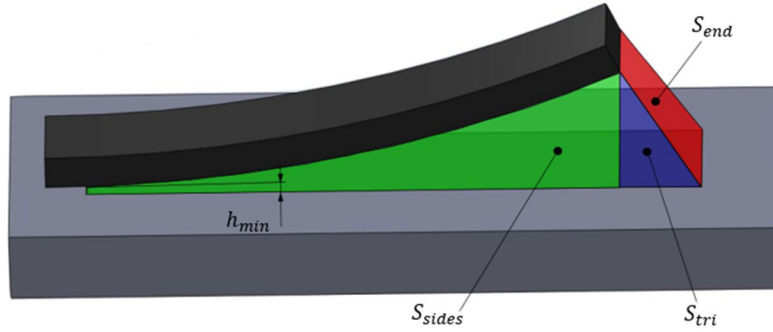


Figure 14. Useful section of airflow under a blown open free reed.

This model also includes the side areas and the two remaining triangles (Figure 13.). Moreover, the clearance gap between the reed and its support, the rotation of the cross section at the end of the beam and the thickness of the beam are also taken into consideration.

The vertical displacement of the neutral section of the reed $y_n(x, t)$ can be calculated using the mode shape defined by equation (5) according to Figure 15:

$$y_n(x, t) = u(x, t) + \frac{h_{reed}}{2} = \alpha_n(t) \cdot \psi_1(x) + \frac{h_{reed}}{2} \quad (49)$$

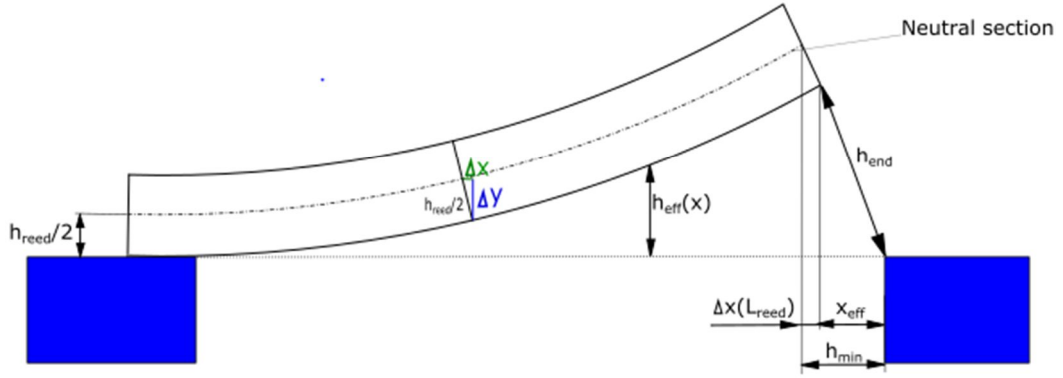


Figure 15. Geometrical parameters for calculating the useful section

After getting the displacement of the neutral section, the coordinates of the upstream and downstream sections can be calculated as we know that the cross sections are always perpendicular to the neutral section (Figure 15.)

$$\Delta y(x, t) = \frac{h_{reed}}{2} \cdot \frac{L_{reed}}{\sqrt{L_{reed}^2 + (u'(x, t) \cdot L_{reed})^2}} \quad (50)$$

$$\Delta x(x, t) = \frac{h_{reed}}{2} \cdot \frac{u'(x, t) \cdot L_{reed}}{\sqrt{L_{reed}^2 + (u'(x, t) \cdot L_{reed})^2}} \quad (51)$$

The upstream and downstream displacements can also be calculated

The transverse displacement of the upstream section: $h_{up}(x, t) = y_n(x, t) - \Delta y(x, t)$

The transverse displacement of the downstream section: $h_{dn}(x) = y_n(x, t) + \Delta y(x, t)$

The x displacement of the upstream section: $x_{up}(x, t) = x_n(x, t) + \Delta x(x, t)$

The x displacement of the downstream section: $x_{dn}(x) = x_n(x, t) - \Delta x(x, t)$

where $x_n(x, t)$ is the axial coordinate of the neutral section.

In case of a blown open reed, h_{eff} equals to the transverse displacement of the upstream section and x_{eff} can be calculated from the clearance gap (h_{min}) and the x displacement of the upstream section at the end of the reed ($\Delta x(L_{reed})$)

Therefore, h_{end} can be calculated:

$$h_{end}(t) = \sqrt{h_{eff}(L_{reed}, t)^2 + (h_{min} - \Delta x(L_{reed}, t))^2} \quad (52)$$

S_{end} can be calculated as an area of a trapezoid:

$$S_{end}(t) = h_{end}(t) \cdot (b + h_{min}) \quad (53)$$

The side areas can be calculated with the following formula:

$$S_{sides}(t) = 2 \cdot \int_0^{L_{reed}} \sqrt{h_{eff}(x,t)^2 + h_{min}^2} \quad (54)$$

The area of the remaining triangle:

$$S_{tri}(t) = h_{eff} \cdot (h_{min} - \Delta x(L_{reed}, t)) \quad (55)$$

The area of the useful section depending on the y coordinate of the end of the reed, according to Millot and Baumann can be seen in Figure 16, drawn with blue line.

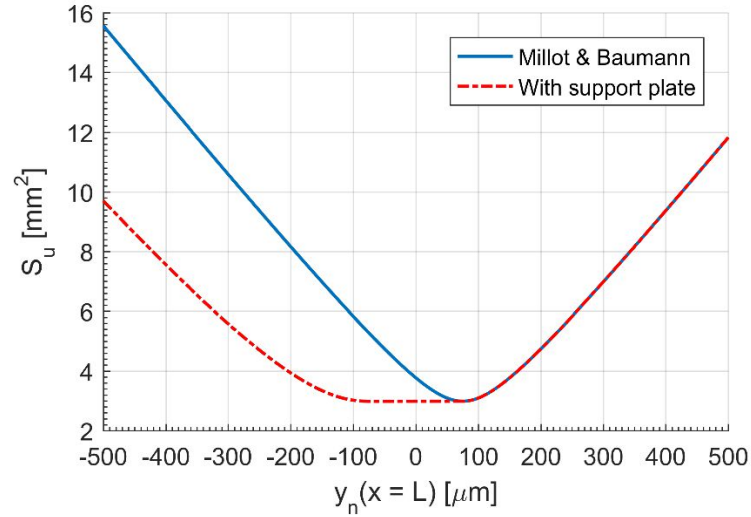


Figure 16. Useful section of an example reed.

It can be seen, that the minimum of the function is shifted from the $y = 0$ location, because of the offset of the neutral section.

On the other hand, the original model does not take the width of the support into account. The value of the useful section is almost constant from the position it becomes flat (position 1 in Figure 17) until it reaches the inner surface of the support (position 2 in Figure 17).

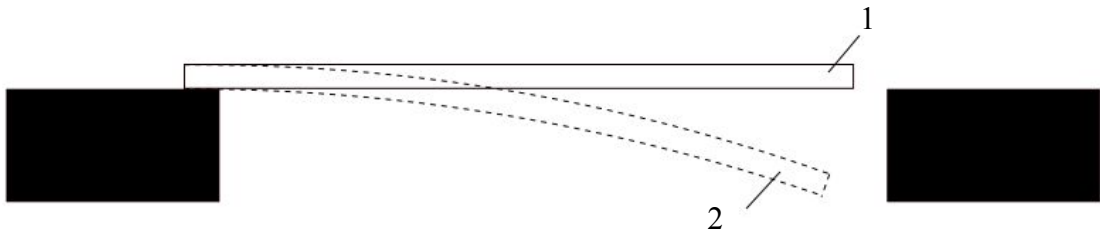


Figure 17. The effect of the tongue holder plate on the useful section.

Therefore the useful section depending on the y coordinate of the tip of the reed can be seen in Figure 16, marked with red dashed line.

4. COMPUTER MODEL

4.1. Reed vibration by modal superposition

The vibration of the reed can be calculated using modal superposition based on the theory that can be read in Section 3.2.

$$u(x, t) = \sum_{n=1}^{\infty} \psi_n(x) \cdot q_n(t) \quad (56)$$

Where $q_n(t)$ are the modal coordinates. Substituting equation (56) into the beam motion equation (1) we get the following equation:

$$g(x, t) - EI \sum_{n=1}^{\infty} \psi_n^{(4)}(x) \cdot q_n(t) = \rho \cdot A \cdot \sum_{n=1}^{\infty} \psi_n(x) \cdot \ddot{q}_n(t) \quad (57)$$

Where the fourth derivative of the eigenmodes with respect to x can be expressed as:

$$\psi_n^{(4)}(x) = \frac{\rho A}{IE} \omega_n^2 \cdot \psi_n(x) \quad (58)$$

Therefore the motion equation can be written in the following form:

$$g(x, t) - \rho A \sum_{n=1}^{\infty} \omega_n^2 \cdot \psi_n(x) \cdot q_n(t) = \rho \cdot A \cdot \sum_{n=1}^{\infty} \psi_n(x) \cdot \ddot{q}_n(t) \quad (59)$$

The motion equation can be projected onto the $\psi_m(x)$ eigenmode by taking the scalar product of $\psi_m(x)$ and the equation:

$$\begin{aligned} \langle \psi_m(x), g(x, t) \rangle - \langle \psi_m(x), \rho A \sum_{n=1}^{\infty} \omega_n^2 \cdot \psi_n(x) \cdot q_n(t) \rangle = \\ \langle \psi_m(x), \rho A \sum_{n=1}^{\infty} \psi_n(x) \cdot \ddot{q}_n(t) \rangle \end{aligned} \quad (60)$$

where $\langle f_1(x), f_2(x) \rangle = \int_0^L f_1(x) \cdot f_2(x) dx$ is the scalar product of two functions. (That is the Lebesgue integral of the product of the two functions.)

As the mode shapes are orthogonal and normalized, equation (60) can be simplified:

$$g_m(t) - \rho A \omega_m^2 q_m(t) = \rho A \ddot{q}_m(t) \quad (61)$$

where: $g_m(t) = \langle \psi_m(x), g(x, t) \rangle$ is the modal force density.

Equation (61) can be written in the following form:

$$f_m(t) - \omega_m^2 q_m(t) = \ddot{q}_m(t) \quad (62)$$

Where $f_m(t) = \frac{g_m(t)}{\mu}$ is the modal force density over unit mass and $\mu = \rho A$ is the mass over unit length.

If the damping of the reed is also taken into consideration, we get the following equation:

$$f_m(t) - \omega_m^2 q_m(t) - 2\xi_m \omega_m \dot{q}_m = \ddot{q}_m(t) \quad (63)$$

Expressing the damping by the quality factor (equation (23)):

$$f_m(t) - \omega_m^2 q_m(t) - \frac{\omega_m}{Q_m} \dot{q}_m = \ddot{q}_m(t) \quad (64)$$

Equation (64) can be written in the following form:

$$\begin{bmatrix} \ddot{q}_m \\ \dot{q}_m \end{bmatrix} = \begin{bmatrix} -\frac{\omega_m}{Q_m} & -\omega_m^2 \\ 1 & 0 \end{bmatrix} \cdot \begin{bmatrix} \dot{q}_m \\ q_m \end{bmatrix} + \begin{bmatrix} f_m(t) \\ 0 \end{bmatrix} \quad (65)$$

Introducing the state space vector $\mathbf{x}_m(t) = [\dot{q}_m(t) \ q_m(t)]^T$ the calculation can be converted into the following form:

$$\dot{\mathbf{x}}_m(t) = \begin{bmatrix} -\frac{\omega_m}{Q_m} & -\omega_m^2 \\ 1 & 0 \end{bmatrix} \cdot \mathbf{x}_m(t) + \begin{bmatrix} f_m(t) \\ 0 \end{bmatrix} \quad (66)$$

Therefore, the equation is written in the form of a general Cauchy–Euler equation:

$$\dot{\mathbf{x}}(t) = \mathbf{A}\mathbf{x}(t) + \mathbf{f}_e(\mathbf{x}, t) \quad (67)$$

These types of equations can be solved using the “ODE45” differential equation solver of Matlab. [MathWorks ODE45, 2016]

The jet velocity can also be defined according to section 3.4.1 for the first calculations, the simplified useful section is used (according to formula (48)).

The opening at the tip of the reed can be calculated if the vibration is known:

$$h(t) = \sum_{i=1}^{\infty} \psi_i(L) \cdot q_i(t) \quad (68)$$

The flow volume of the jet:

$$U(t) = S(t) \cdot v(t) \quad (69)$$

The derivative of the volume flow with respect to time will be needed for the calculations of the coupling with the resonator:

$$\frac{dU(t)}{dt} = \frac{dS(t)}{dt} \cdot v(t) + S(t) \cdot \frac{d(v)}{d(t)} \quad (70)$$

The velocity of the jet and its time derivative still needs to be calculated. The velocity can be calculated using Bernoulli’s law (46). The derivative of the velocity with respect to time:

$$\frac{dv(t)}{dt} = \sqrt{\frac{2}{\rho_0}} \cdot \frac{1}{2\sqrt{p_0 - p(t)}} \cdot \left(-\frac{\partial p}{\partial t} \right) \quad (71)$$

For the second simulation, the useful section is calculated according to Section 3.4.2.

4.2. Resonator representation

4.2.1. MODAL SUPERPOSITION

In the first simulation approach, the modal superposition is used to describe the resonator. The sound pressure can be calculated from the input impedance as follows. The input impedance can be written in the following form using modal superposition:

$$Z_{in}(\omega) \cong \sum \frac{j\omega F_j}{\omega_j^2 - \omega^2 + \frac{\omega_j}{Q_j}\omega} = \frac{P(\omega)}{U(\omega)} \quad (72)$$

Where

- Q_j is the quality factor of the j -th eigenmode
- F_j is the modal weight of the j -th eigenmode
- ω_j is the eigenfrequency of the j -th eigenmode

In this model the calculation is simplified by truncating the series at n -th order, and the remaining part is neglected. According to this simplification, this method is called “impedance truncation method”.

The equation is true to the summands as well for example:

$$\frac{j\omega F_j}{\omega_j^2 - \omega^2 + \frac{\omega_j}{Q_j}\omega} = \frac{P_j(\omega)}{U(\omega)} \quad (73)$$

The form of equation (73) in the time domain:

$$F_j \cdot \frac{dU}{dt} = \omega_j^2 p_j(t) + \frac{d^2 p_j(t)}{dt^2} + \frac{dp_j(t)}{dt} \cdot \frac{\omega_j}{Q_j} \quad (74)$$

Equation (74) can be written as a system of two ordinal differential equations:

$$\begin{bmatrix} \ddot{p}_j \\ \dot{p}_j \end{bmatrix} = \begin{bmatrix} -\frac{\omega_j}{Q_j} & -\omega_j^2 \\ 1 & 0 \end{bmatrix} \cdot \begin{bmatrix} \dot{p}_j \\ p_j \end{bmatrix} + \begin{bmatrix} F_j \cdot \frac{dU}{dt} \\ 0 \end{bmatrix} \quad (75)$$

Where the Quality factor Q_j be calculated using the 3 dB method (see in section: 3.3.2). Equation (75) can also be converted into the Cauchy–Euler form, and solved using “ODE45” solver of Matlab. p and \dot{p} (the pressure and its derivative with respect to time) are attained using modal superposition as

$$p(t) = \sum_{j=1}^n p_j(t) \quad (76)$$

$$\dot{p}(t) = \sum_{j=1}^n \dot{p}_j(t) \quad (77)$$

4.2.2. REFLECTION FUNCTION

In the second simulation approach, the so-called reflection function is used for calculating the pressure inside the resonator. The reflection coefficient $R(f)$ with frequency f can be calculated from the input impedance $Z_{in}(f)$ and characteristic impedance Z_0 of the resonator. [Schumacher, 1983; Hikichi et al, 2003]

$$R(f) = \frac{Z_{in}(f) - Z_0}{Z_{in}(f) + Z_0} \quad (78)$$

The reflection function $r(t)$ is defined by the inverse Fourier transform of $R(f)$. It represents the pressure waveform which is reflected back from the remote end of the resonator in case of a pressure impulse excitation at $t = 0$.

The pressure can be calculated using the reflection function as

$$p(t) = Z_0 \cdot U(t) + r(t) * (p(t) + Z_0 U(t)) \quad (79)$$

The second part of this expression is a convolution, which means that its value at a certain time instant is dependent from the past quantities:

$$r(t) * (p(t) + Z_0 U(t)) = \int_0^t r(\tau) \cdot (p(t - \tau) + Z_0 U(t - \tau)) d\tau \quad (80)$$

The volume flow can be expressed using Bernoulli's law (Section 3.4.1) according to Equations (46) and (47).

Using time discretisation, equation (80) can be written in the following form:

$$p[n] = Z_0 \cdot U[n] + \sum_{k=0}^n r[k] \cdot (p[n - k] + Z_0 U[n - k]) \quad (81)$$

where $t = n \cdot \Delta t$ (Δt is the time step)

The convolution sum can be expressed as an aggregate of a sum that only contains the past and a product that contains the present:

$$p[n] = Z_0 U[n] + \sum_{k=1}^n r[k] (p[n - k] + Z_0 U[n - k]) + r[0] (p[n] + Z_0 U[n]) \quad (82)$$

The discrete form of the volume velocity:

$$U[n] = S_u[n] \cdot \sqrt{\frac{2}{\rho_0}} \sqrt{|p_0 - p[n]|} \cdot \text{sign}(p_0 - p[n]) \quad (83)$$

Substituting this expression into equation (82):

$$\begin{aligned} p[n] \cdot (1 - r[0]) - Z_0 \cdot S_u[n] \cdot \sqrt{\frac{2}{\rho_0}} \cdot \sqrt{|p_0 - p[n]|} \cdot \text{sign}(p_0 - p[n]) \cdot (1 + r[0]) \\ - \sum_{k=1}^n r[k] \cdot (p[n - k] + Z_0 U[n - k]) = 0 \end{aligned} \quad (84)$$

Equation (90) can be solved for $p[n]$ using the "fsolve" function of Matlab for each n .

4.3. Iterative solution

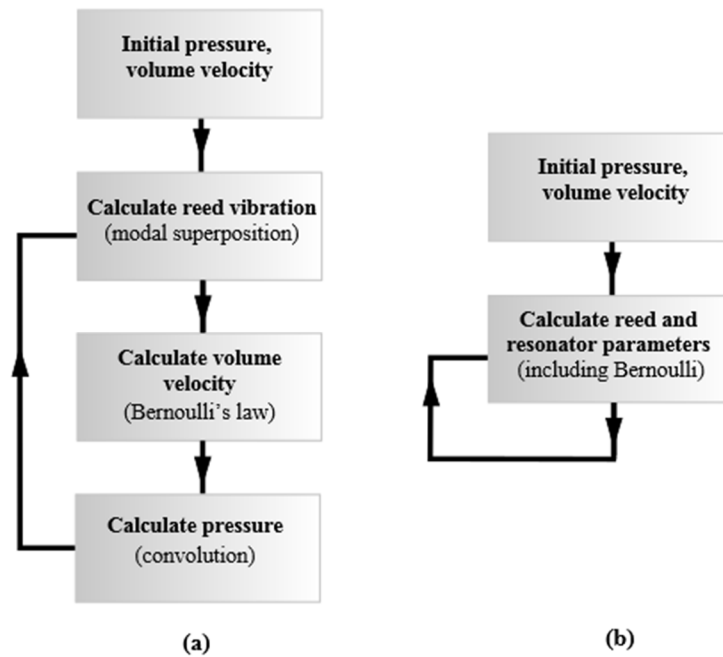


Figure 18. Iteration (a):reflection function method, (b): truncated impedance method

The equations of Section 4 were implemented in Matlab. The simulations are performed using iterations as depicted in Figure 18 to calculate the solution of the system in each time step. Using the reflection function method, the equation of the reed vibration and the velocity is calculated in different steps, while the truncated impedance method solves the equation of the coupled system consisting of equations (66) and (75).

5. RESULTS

In this section the results of the computer simulations are presented. First, in Section 5.1 a test geometry is used in order to demonstrate the behaviour of the implemented modeling approaches. The two different resonator representations (impedance truncation and reflection function) are compared for this test pipe with different feedback strengths. Typical features of the results are explained by references to the underlying physical mechanisms of the sound generation process. Second, in Section 5.2 the results for the experimental pipes are presented and compared to the measurement results regarding various aspects.

5.1. Validation of the modeling methodology

For testing the simulations and to examine the behaviour and consistency of the implemented computer models a virtual pipe was used that consists of a blown open reed connected to a simple conical resonator. The parameters are the following:

- density of the reed: $8860 \frac{\text{kg}}{\text{m}^3}$
- elasticity modulus of the reed: 97.63 GPa
- length of the reed: 28 mm
- width of the reed: 3.7 mm
- thickness of the reed: 0.05 mm
- radius of the resonator: 20 mm
- length of the resonator: 400–600 mm
- overpressure in pressure tank: 500 Pa

5.1.1. REED VIBRATION

The mode shapes of the reed can be seen in Figure 19. The derivatives of the mode shapes with respect to x are shown in Figure 20. From the figures, it can be seen, that (1) both the displacement and its derivative are zero at the clamped end of the reed and

(2) the second derivative of the mode shapes at the free end of the reed is zero, therefore, all boundary conditions elaborated in Section 3.2 are satisfied by the mode shapes.

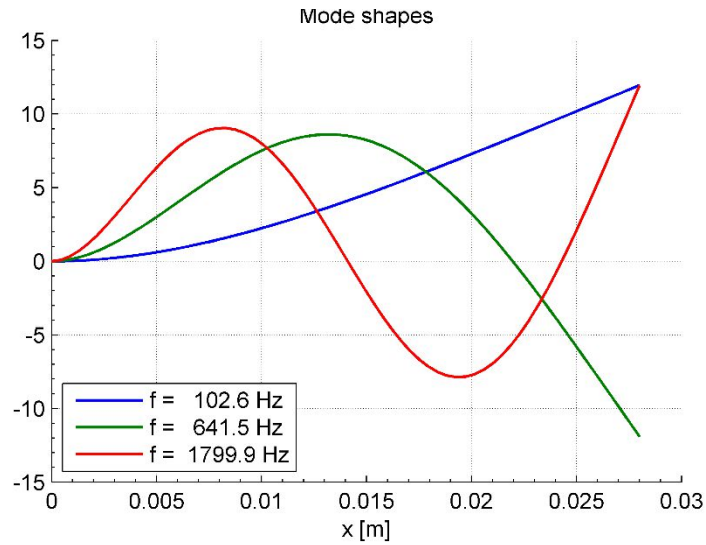


Figure 19. Mode shapes and eigenfrequencies of the example reed

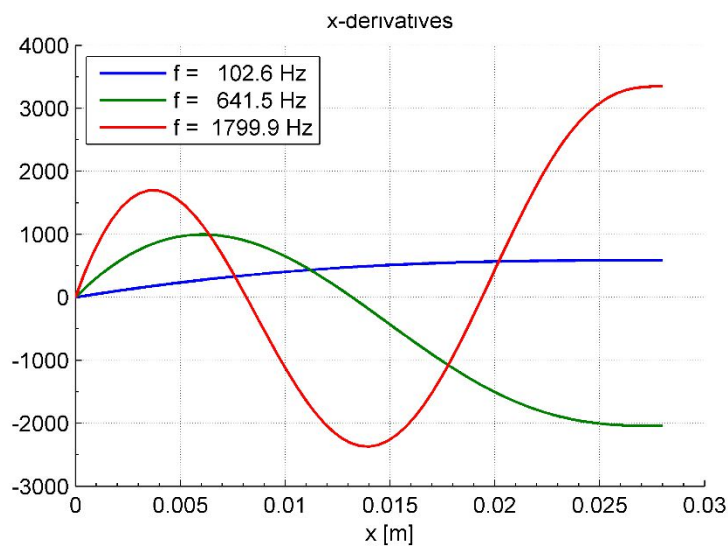


Figure 20. The x -derivatives of the example mode shapes

5.1.2. RESONATOR

The input impedance of the resonator (normalised by the acoustical impedance of the plain wave) can be seen in Figure 21. The resonance frequencies are denoted by the local maxima of the function.

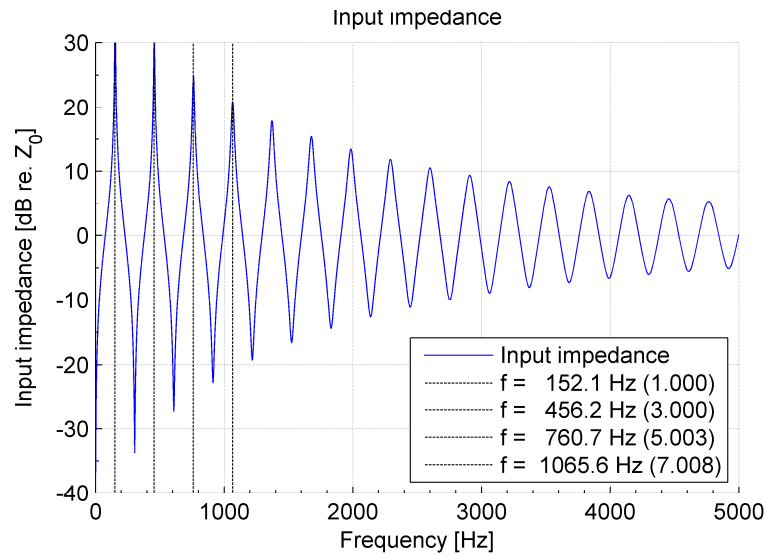


Figure 21. Input impedance of the example resonator with length $L = 550$ mm

It can also be seen in Figure 21 that the peaks are getting wider with the mode number, therefore the quality factors are decreasing. That means that the damping is getting greater as the frequency is increasing.

According to the solution of the equations of the sound field, the eigenfrequencies should be the odd multiples of the first eigenfrequency. On the other hand, the peaks are not exactly at these frequencies. For example the ratio of the third and the first eigenfrequency is 5.003 instead of 5, the ratio of the fourth and the first eigenfrequency is 7.008 instead of 7, and so on. The difference between the theoretical frequencies and the calculated frequencies are growing with increasing the frequency. This inharmonicity can be explained by the fact, that the radiation impedance and the associated length correction are frequency dependent. The same phenomenon is observed in case of open labial organ pipes, see e.g. [Miklós and Angster, 2000].

5.1.3. IMPEDANCE TRUNCATION

The reduced input impedance function is displayed in Figure 22. In this example the input impedance is truncated to 5 modes.

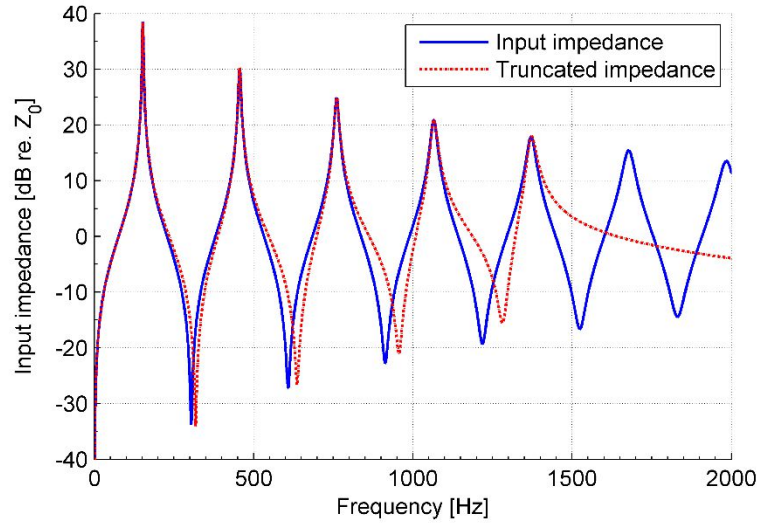


Figure 22. Truncated input impedance of the example resonator with $L = 550$ mm

It can be seen, that the reduced impedance function is a good approximation of the calculated impedance function in the low frequency range. As the function is fitted to the peaks of the calculated input impedance, it gives a good approximation around them. On the other hand, local minima of the function are shifted from the original function.

5.1.4. REFLECTION FUNCTION

The sound pressure can be calculated with the help of the impulse response function $G(t)$, the pressure response of the system in case of a Dirac-delta volume velocity excitation, using convolution:

$$p(t) = G * U \quad (85)$$

As convolution is an integral, equation (85) can be written in the following form:

$$p(t) = \int_0^{\infty} G(\tau) \cdot U(t - \tau) d\tau \quad (86)$$

This numerical integration is computationally quite intensive, as the impulse response function is a slowly decaying function of time, as illustrated in Figure 24 for the case of the example pipe.

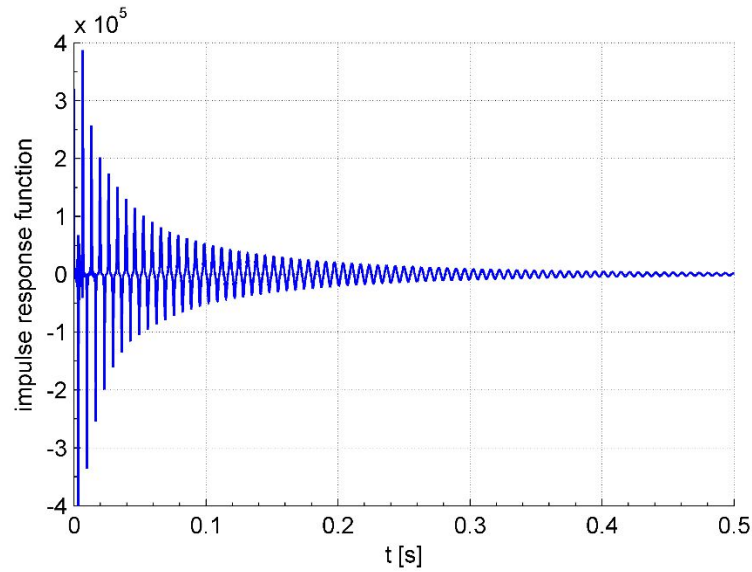


Figure 23. Impulse response function of the example pipe.

The sound pressure can also be calculated with the help of the reflection function (see Section 4.2.2):

$$p(t) = Z_0U + r * (p + Z_0U) \quad (87)$$

As the reflection function decays to zero much faster than the impulse response function (Figure 25), the calculation of this convolution is much faster.

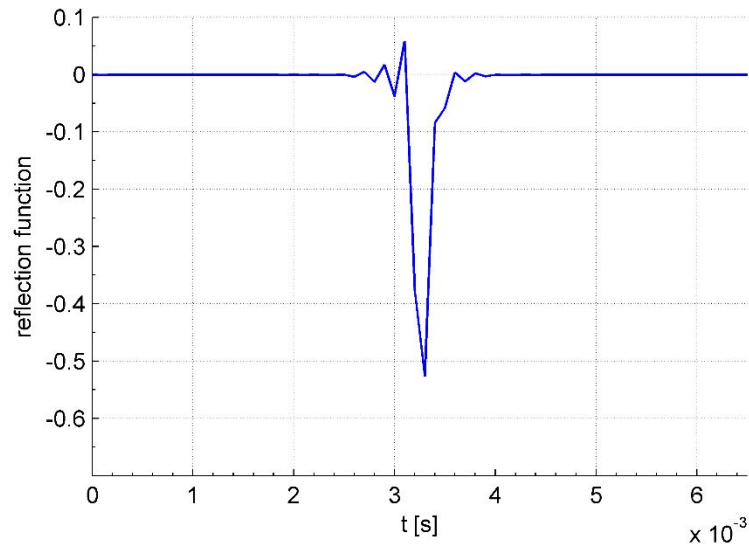


Figure 24. Reflection function of the example resonator

On the other hand, in case of using the reflection function in the convolution integral, the main difficulty is to find the way to eliminate the error caused by using Fast Fourier Transformation. The problems stem from not choosing the maximal frequency of the

calculated input impedance f_{max} correctly [Gazengel, 1995]. Gazengel, Gilbert and Amir noticed that the shape of the reflection function is highly affected by f_{max} . If it is chosen to be the on a zero point of the input impedance, the resulting reflection function is rippled, as shown in Figure 25. On the other hand, if it is chosen to be one of the natural resonance frequencies of the resonator, the ripple nearly disappears (Figure 24).

It can also be seen in Figures 24 and 25 that the position of the peak of the reflection function is equal to the period of the first eigenfrequency of the resonator, as this is exactly the amount of time that the pressure wave has to travel to get back to the point of the excitation after being reflected from the open end. Because of the open end, the reflected pressure pulse suffers a 180° phase shift. That is why the reflection function has a negative peak.

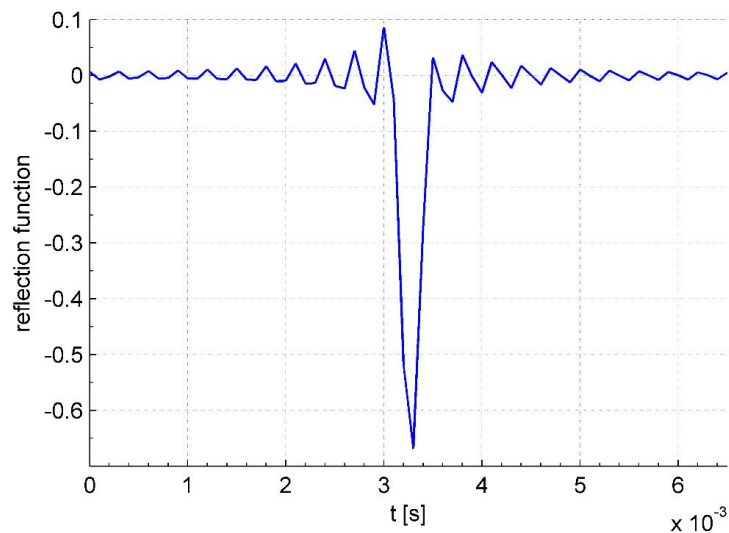


Figure 25. Rippled reflection function due

5.1.5. EXTREMAL CASES

As the sound pressure is reflected back from the open end of the resonator in the opposite phase, if the length (L) of the resonator is close to $L = \frac{\lambda}{2}n$ where λ is the wavelength of the wave having the same frequency as the reed vibration, and n is a positive integer number, the reflected sound pressure wave works as a negative feedback, and prevents the reed from vibrating. If the length of the resonator is close to $L = \frac{\lambda}{4}(2n + 1)$ the reflected wave works as a positive feedback and boosts the vibration of the reed.

The sound pressure and the displacement of the reed can be seen in Figures 26 and 27 in case of $L = 400$ mm. The reed has a stable displacement from the time when the exciting pressure is applied but oscillation does not occur. After the opening of the reed, the static pressures equalize and the acoustic pressure remains zero until the end of the simulation.

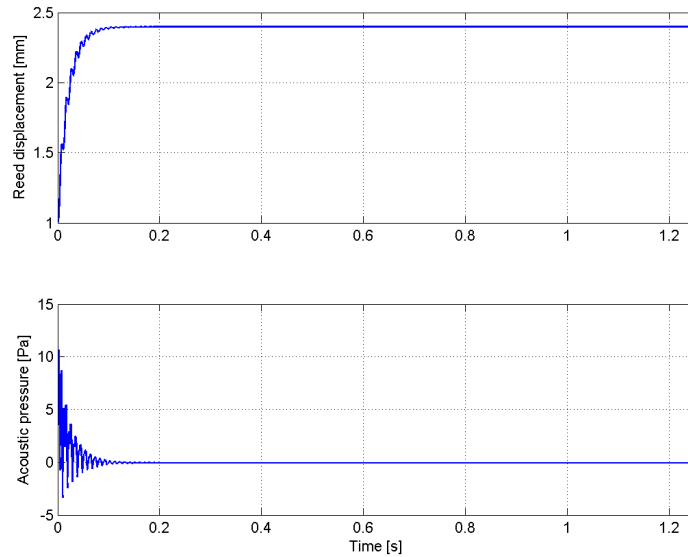


Figure 26. Acoustic pressure and reed displacement in case of negative feedback (reflection function method)

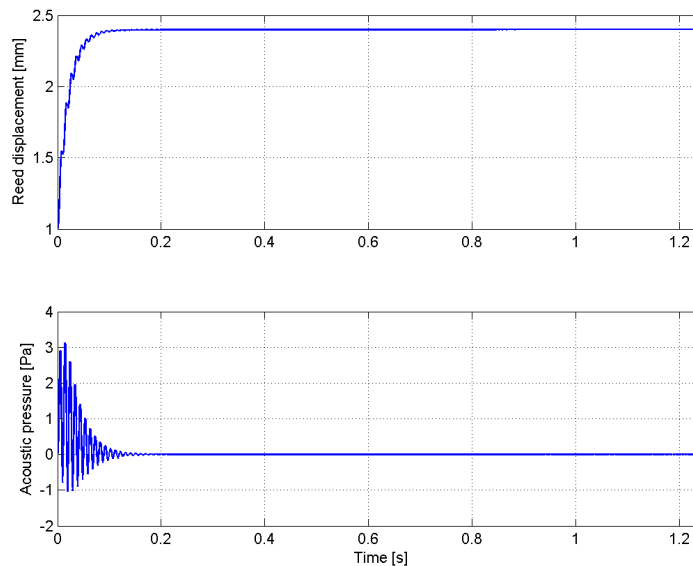


Figure 27. Acoustic pressure and reed displacement in case of negative feedback (impedance truncation method)

It can be seen in Figures 26 and 27 that there is a difference between the transient vibrations, but the final reed displacement and the pressure will be the same in case of both methods.

In case of choosing the resonator length $L = 600$ mm, positive feedback is attained and the reed and the acoustic pressure are starting to oscillate with an increasing amplitude. The results are shown in Figures 28 and 29. It can be seen, that the steady state results are quite similar in this case as well. The central value of the oscillation is the same with both methods. The amplitudes are also the same. However, there is a little difference between the transient vibrations. It can be seen, that it takes the impedance truncation method to come to a steady state vibration.

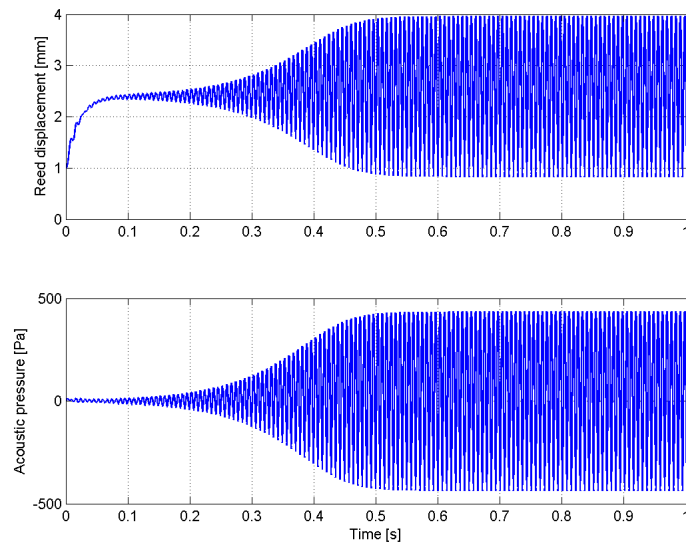


Figure 28 Reed displacement and acoustic pressure in case of positive feedback
(reflection function method)

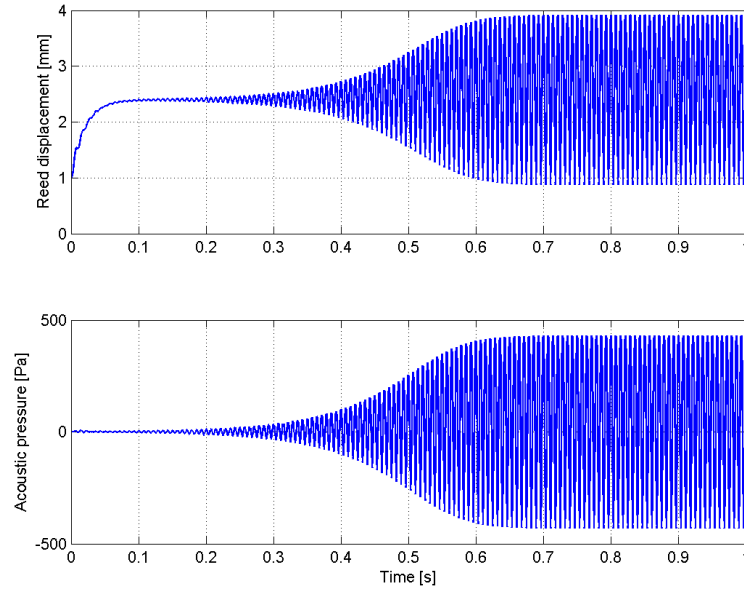


Figure 29 Reed displacement and acoustic pressure in case of positive feedback (impedance truncation method)

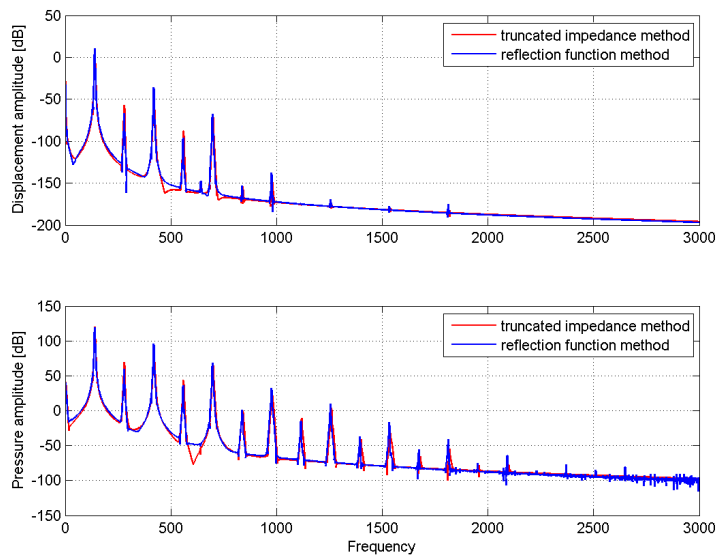


Figure 30. Spectrum of the reed displacement and the Pressure amplitude (the results of the reflection function method are marked with red line, while the results of the truncated impedance is marked with blue line)

The spectrum of the reed vibration and the acoustic pressure are displayed in Figure 30. As it can be seen the spectra are similar in case of the different simulation methods. This shows that the eigenfrequencies (therefore the timbre of the pipe) are independent from the resonator representation, therefore, both methods represent the sound propagation properly. It can also be seen in the spectrum of the reed vibration, that the first ei-

genfrequency is the dominant one in the vibration as the first peak is more than 40 dB higher than the other ones. That is why the movement of the reed is sufficiently represented by its first eigenmode and its further eigenfrequencies can be neglected.

5.2. Simulation of the experimental pipes

The construction of the experimental pipes were shown in Figure 4 earlier. The parameters of the tongues and resonators of experimental pipes #1, #2 and #3 are listed in Tables 1 and 2. These parameters were also used in the simulations presented in this section.

	length [mm]	width [mm]	height [mm]	density [kg/m]	elasticity modulus [GPa]	clearance gap [mm]	frequency [Hz]	Quality factor [-]
1	21.19	2	0.2	8860	105	0.05	247.8	151.8
2	25.62	2	0.15			0.05	127.1	218.5
3	47.53	5	0.4			0.1	98.5	108.0

Table 1. Parameters of the tongues of the experimental pipes

	Physical length [mm]	Inner circumference [mm]	Effective radius [mm]	Effective length [mm]	Frequency [Hz]	quality factor [-]
1	597	56	7.9	610	284.4	44.2
2	1181	113.3	16	1207	143.7	62.1
3	1188	63.9–172-9	9–24.4	1170	110.5	50.8

Table 2. Parameters of the resonators of the experimental pipes

5.2.1. COMPARISON OF STATIC PARAMETERS

First, two important parameters of the pipes are compared to the measured results. These are (1) the minimal blowing pressure required to obtain a stable oscillation and (2) the fundamental frequency of the pipe sound.

The minimal overpressures are shown in Table 3. Both simulation methods gave the same results in case of all pipes, which are only slightly different from the measured ones.

Minimal overpressure [Pa]		
	Measurement	Simulation (both methods)
Pipe 1	265	260
Pipe 2	220	220
Pipe 3	195	200

Table 3. Minimal blowing pressures required for stable sound

Frequency of the sound [Hz]			
	Measurement	Simulation (impedance truncation)	Simulation (reflection function)
Pipe 1	278.4	283.5 (+31 cents)	281.9 (+22 cents)
Pipe 2	139.8	145.5 (+70 cents)	145.3 (+66 cents)
Pipe 3	108.9	111.6 (+41 cents)	111.3 (+36 cents)

Table 4. Steady state frequencies compared to the measured values.

(The numbers in the brackets indicate the deviations from the measured frequencies.)

The fundamental frequencies of the simulated reed vibrations and sounds displayed in Table 4 were calculated from the steady state part of the simulated reed displacement signal. To achieve accurate detection of the frequency, the signals were filtered and a sinus-fit algorithm was used. This method gives a greatly enhanced accuracy of the frequency detection compared to the standard FFT-based method.

It can be seen in Table 4, that the frequencies of the simulations are a little higher than the measured values. The difference can be caused by the fact, that the excitation pressure is assumed to be constant in the simulations, while in reality, the excitation pressure is also wavering. Moreover, the air in the pressure tank is also coupled to the resonator, therefore it is tuning the resonators for a slightly different frequency.

5.2.2. TRANSIENT VIBRATION

The sound pressure of pipe 1 (at the position of the reed) can be seen in Figure 31. It shows, that in the transient section not only the amplitude of the oscillation changes, but the waveform is modified as well. Similar results were found in case of the other pipes as well.

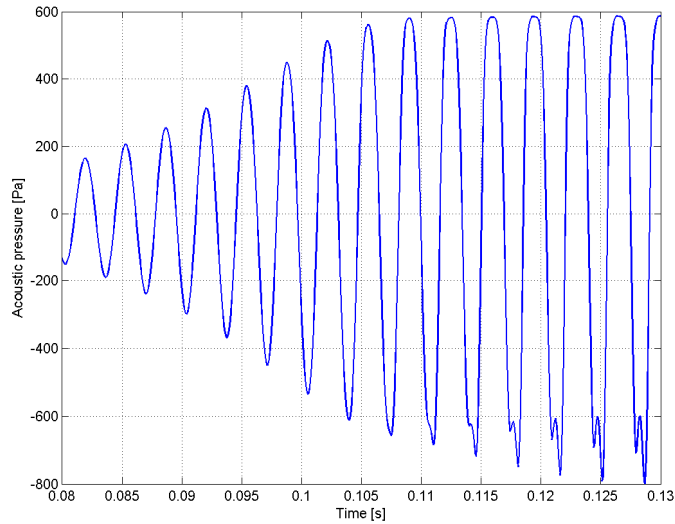


Figure 31 Transient oscillation of sound pressure (pipe 1)

5.2.3. IMPEDANCE TRUNCATION VERSUS REFLECTION FUNCTION

The input impedances of the experimental pipes calculated by the model introduced in Section 3.3.4 can be seen in Figures 32–34. It can be seen, that the input impedances are much different from the simple conical resonator's impedance. It can be seen in Figure 33 that in certain frequencies (for example around 1050 Hz and 3050 Hz) the reflection from the open end and the reflection of the closed end work as a negative feedback therefore there is a drastic change in the impedance function that occurs periodically. This effect was also experienced during the measurements. In case of pipes #1 and #2 there are smaller sharp peaks in the input impedance between the highest peaks. These are due to the asymmetric position of the reed along the length of the resonator.

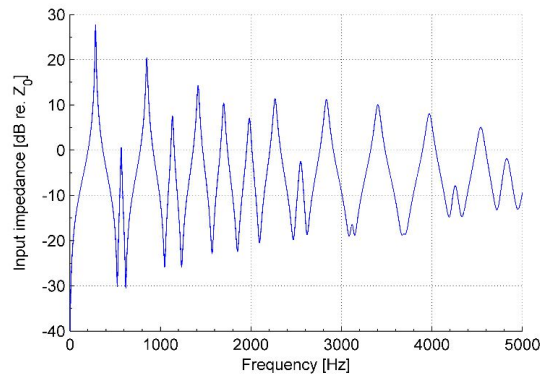


Figure 32. Input impedance of Pipe 1

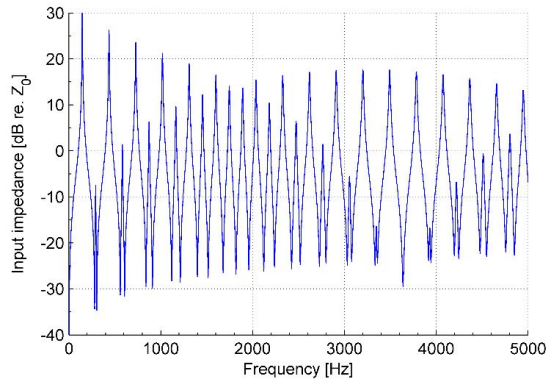


Figure 33. Input impedance of Pipe 2

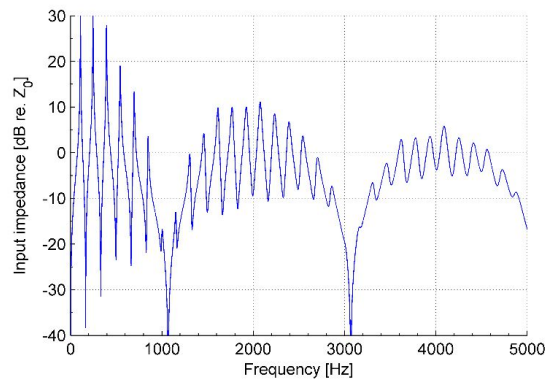


Figure 34. Input impedance of Pipe 3

The reflection functions of the experimental pipes can be seen in Figure 35. They are much complex than the reflection function of a simple conical resonator, because the reeds are not located at the end of the resonator. Therefore, there are reflections from both ends and the functions have more peaks than the one in shown in Figure 24.

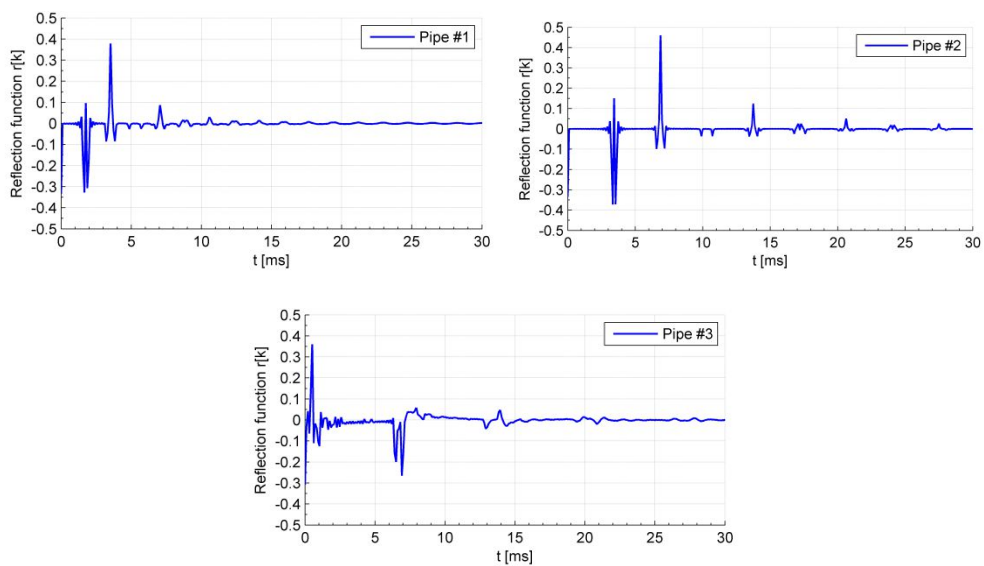


Figure 35 Reflection functions of the experimental pipes

5.2.4. THE EFFECT OF THE TRUNCATION

In order to examine the effect of the truncation parameter on the resulting steady state characteristics of the oscillations, the impedance truncation simulations were run taking different amount of resonator modes into account. Simulations were performed for pipe 1 with a blowing pressure of $P_0 = 400$ Pa. The results show, that this parameter does not change drastically the resulting frequency. According to Figure 36, taking 5 modes into account gives a really good approximation of the resonator, taking further modes only affects the frequency to a very small extent.

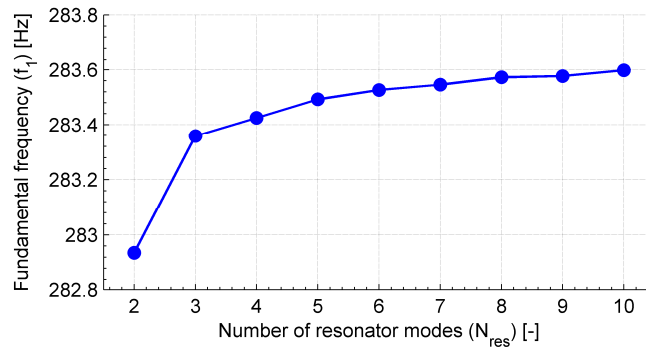


Figure 36. The effect of number of the resonator on the fundamental frequency

5.2.5. CHANGING THE BLOWING PRESSURE

The measurements show that changing the overpressure does not affect the pitch of the pipe, only to a very small extent. Therefore the simulations were run for different overpressures. To be able to compare the change of the pitch of the sounds the resulting frequencies were normalised with the pitch of the 400 Pa overpressure.

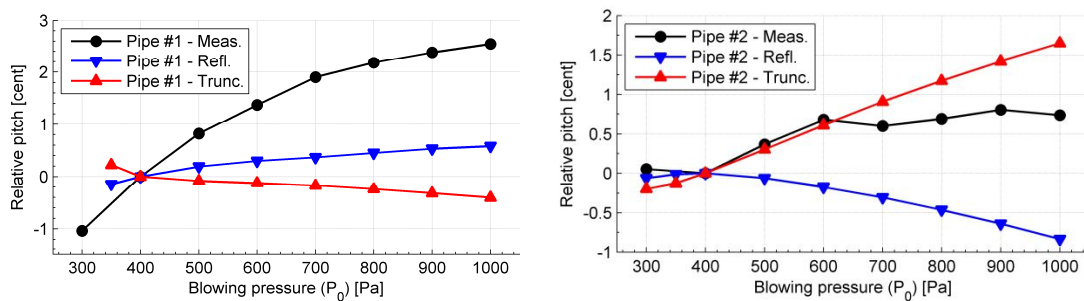


Figure 37. The effect of the overpressure on the pitch

Figure 37 contains the relative pitches of the two simulations and the measurement for pipe 1 and 2. It can be seen, that the change of the pitch is few cents, what is a very small (almost non-audible) difference. It should also be noted that half degree change of the ambient temperature also detunes the pipes about 2 cents.

The simulations for pipe 3 gave unexpected results. When the blowing pressure reaches 500 Pa, the frequency of the sound undergoes a significant change. Moreover, the change of the overpressure modifies the waveform of the sound pressure as well, as shown in Figure 38. Such effects were not experienced in the measurements and thus, they can be thought of as unphysical. At this stage this strange phenomenon occurring only in case of pipe 3 is unexplained.

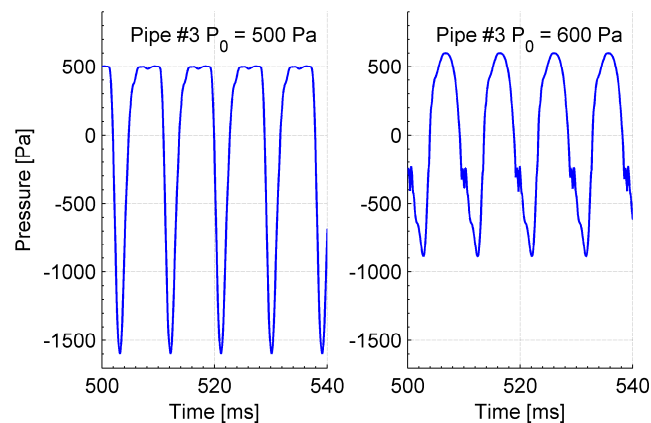


Figure 38. The effect of the overpressure on the waveform of the sound pressure

The effects of changing the blowing pressure on the spectrum of the pressure waveforms at the reed position were also investigated. The spectra were evaluated in the steady state of the sound production. Then, the envelopes (i.e. the curves containing solely the amplitude of the harmonic partials) were evaluated. The resulting envelopes are displayed in Figures 39 (impedance truncation method) and Figure 40 (reflection function method). It can be seen in the figures that the amplitudes are increasing with the blowing pressure, as expected. Furthermore, higher harmonics become more and more enhanced compared to the fundamental with increasing the overpressure. This means that the timbre of the sound is changing significantly. Although these envelopes are evaluated at the point of the reed, similar results can be expected at the open end of the resonator as the transfer from the reed position to the open end is characterized by a simple (linear, amplitude independent) transfer function, see equation (37). These results are also in good agreement with the measurements.

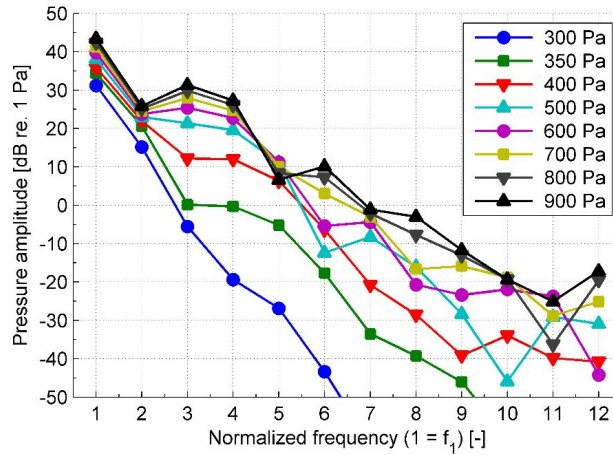


Figure 39. The effect of the overpressure on the harmonics (impedance truncation method)

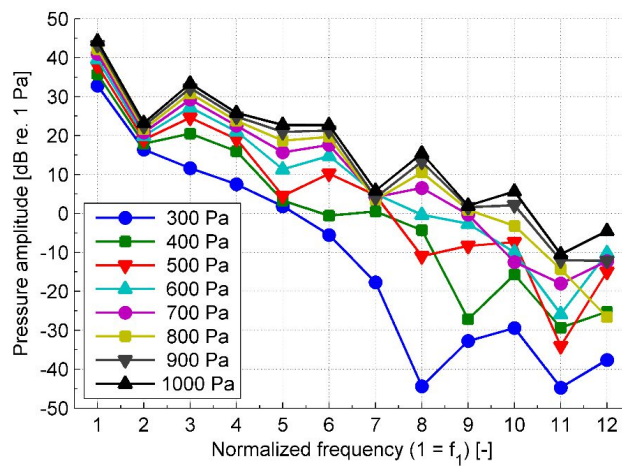


Figure 40. The effect of the overpressure on the harmonics (reflection function method)

By comparing the two simulation approaches, it is seen that in case of the truncated impedance method, the higher harmonics have smaller pressure amplitudes. This is caused by the truncation of the resonator modes. On the other hand, the reflection function implicitly contains all modes under the half of the sampling frequency, therefore the higher frequency contents of the resulting sounds are also enhanced. Beside these small dissimilarities, the two methods give sounds and spectral envelopes that are very much alike.

6. CONCLUSION

During our work, a simplified model of the sound production of a novel organ pipe construction with a blown-open free reed was elaborated by connecting the reed vibration to a resonator model through a simplified flow model. The model was improved by making the calculation of the escape area more and more accurate. The useful section model of Millot and Baumann was improved by taking the width of the support into account. Furthermore, it was shown that the free reed model with the useful section can be coupled to a resonator.

The resonator was represented using two different theories: the reflection function and the truncated impedance theory. A simulation of a pipe with simple conical resonator was presented using both methods. The results met the expectation, as both the amplitudes and the central values of the reed displacement and the pressure oscillation were very similar for both methods. Moreover, the spectrum of the oscillations (therefore the pitch of the sound) were almost the same for the two simulations. Small dissimilarities were only observed in the transient signals.

These simulations were also used to describe three experimental pipes with very different resonator shapes. They represented the sound production of the pipes properly. The values of the required pressure of the sound production were really close to the measured ones. The difference between the measured and simulated frequencies can be explained by the fact, that during the simulations the exciting pressure was approximated with a constant while it is not time independent in the reality. Moreover, the effect of the air in the pressure tank was also neglected.

During the measurements it was experienced, that the overpressure does not affect the pitch of the sound; however, it has a significant impact on the timbre of the pipes. This tendency can also be seen from the results of the simulations. It has also been proved, that the motion of the reed is sufficiently represented by its first eigenmode and in case of the truncated impedance method the truncation does not cause a big error. Truncating at the fifth–seventh eigenfrequency gives a really good approximation.

It can be stated that the implemented computer models are correct representations of the experimental pipes. The simulation techniques discussed in the thesis allow rapid com-

putations and the synthesis of sound samples of the pipes too. Despite the simplicity of the applied one-dimensional models, the comparison with the measurements show quite good match.

Further improvements of the models can be done in two main aspects. First, by taking the effects of the pressure tank's air and the time dependent overpressure into account. Second, the simple one-dimensional flow model has the most assumptions that may not be fulfilled under real circumstances. A more precise flow model is expected to enhance the accuracy of the simulations.

REFERENCES

Adachi, S. and Sato, M. "Time-domain simulation of sound production in the brass instrument." *J. Acoust. Soc. Am.* **97**(6), pp. 3850–3861. (1995)

Fiala, P. A hangszerek fizikája. (The physics of musical instruments.) Lecture notes. (2016) Link: <http://last.hit.bme.hu/sites/default/files/documents/hangfiz.pdf> (Last visited 2016. 10. 28.)

Fletcher, N.H.; Rossing, T.D. "The physics of musical instruments" Springer, New York. 2nd Edition, 1998.

Gazengel, B.; Gilbert, J. and Amir, N. "Time domain simulation of single reed wind instrument. From the measured input impedance to the synthesis signal. What are the traps?" *Act. Acust.* **3**, pp. 445–472. (1995)

Hirschberg, A. *et al.* "A quasi-stationary model of air flow in the reed channel of single-reed woodwind instruments." *Act. Acust. united Ac.* **70**(2), pp. 146–154. (1990)

Kinsler, E. L.; Frey, A. R.; Coppers, A. B.; and Sanders, J. V. "Fundamentals of Acoustics." Fourth edition. John Wiley & Sons, Inc., pp 210-233 (2000).

Mathworks Matlab documantation of ODE45 function:

<https://www.mathworks.com/help/matlab/ref/ode45.html> (last visited: 2016. 10. 27.)

McIntyre, M.E.; Schumacher, R.T; Woodhouse, J. "On the oscillations of musical instruments" *J. Acoust. Soc. Am.* **74**(5) pp. 1325-1345, 1983.

Miklós, A.; Angster, J; Pitsch, S. and Rossing; T.D. "Reed vibration in lingual organ pipes without the resonators." *J. Acoust. Soc. Am.* **113**(2), pp. 1081–1091. (2003)

Miklós, A.; Angster, J; Pitsch, S. and Rossing; T.D. "Interaction of reed and resonator by sound generation in a reed organ pipe." *J. Acoust. Soc. Am.* **119**(5), pp. 3121–3129. (2006)

N.H. Fletcher: Autonomous vibration of simple pressure-controlled valves in gas flows. J. Acoust. Soc. Am. **93**(4) pp. 2172–2180 (1993)

Olson, H.F. "Elements of acoustical engineering." Second edition. D. van Nostrand Company, Inc., 1960. p. 116

Rucz, P.; Angster, J. and Miklós, A. "Examination of a novel organ pipe construction with blown open tongue" Proceedings of the DAGA2016, Aachen, Germany. pp. 1292–1295. (2016)

Rucz P. "Innovative methods for the sound design of organ pipes" Ph.D. thesis. Budapest University of Technology and Economics. (2015)

Schumacher, R.T. "Ab initio calculations of the oscillations of a clarinet." Act. Acust. united Ac. **48**(2), pp. 71–85. (1981)

Vaik, I. and Paál, Gy. "Flow simulations on an organ pipe foot model" J. Acoust. Soc. Am. **133**(2) pp. 1102-1110 (2013)

Zacharias, E. "Dynamische Orgelpfeifen" Ars Organi **63** p. 46 (2015)